minerals

MDPI

Article

Sedimentary Filling Evolution under Paleoclimate Transition—A Case Study from the Middle Jurassic Zhiluo Formation, Ordos Basin

Liwei Cui [1,2,3], Nan Peng [1,*], Yongqing Liu [1], Dawei Qiao [1] and Yanxue Liu [1]

[1] The Institute of Geology, Chinese Academy of Geological Sciences, Beijing 100037, China
[2] School of Earth Sciences and Resources, China University of Geosciences, Beijing 100083, China
[3] Cores and Samples Center of Natural Resources, China Geological Survey, Langfang 065201, China
* Correspondence: pengnan19830120@126.com

Abstract: Under a specific tectonic background, the change in paleoclimate can show different facies associations and depositional architecture. The Jurassic China continent was an important region for transforming the Paleotethys tectonic domain to the circum-Pacific tectonic domain, and its paleoclimate information was entirely preserved in the continental sedimentary successions. The Middle Jurassic Zhiluo Formation, in the Ordos Basin, was at just the critical period of paleostructure and paleoclimate transition, preserving considerable sedimentological evidence; however, little sedimentological research has been conducted under the transition. This study reconstructed the sedimentary filling characteristics of the Zhiluo Formation under paleoclimate transition based on field outcrop survey, thin section observation, geochemical indices, stratigraphic correlation, and depositional environment analysis. The results showed that with the paleoclimate change from warm and humid to hot and arid, the sedimentary facies of the Zhiluo Formation were characterised by the change from the braided river/braided river delta in the J_2z^{1-1} sedimentary period to the meandering river/meandering river delta in the J_2z^{1-2} sedimentary period, and finally the change to the meandering river, meandering river delta, and lacustrine in the J_2z^2 sedimentary period. The combined action of the southern super monsoon effect, the increasing global CO_2 concentrations, the moving southward of the East Asian block, and the terrain elevation difference, changed the basin's climate from warm and humid to hot and semi-arid/arid. This study provides a crucial basis for reconstructing the interplay between paleoclimate and paleotectonics, and guiding sedimentology and paleoenvironment research on East Asia during the Middle Jurassic period.

Keywords: jurassic; paleoclimate; facies; tectonics; sedimentary evolution

check for updates

Citation: Cui, L.; Peng, N.; Liu, Y.; Qiao, D.; Liu, Y. Sedimentary Filling Evolution under Paleoclimate Transition—A Case Study from the Middle Jurassic Zhiluo Formation, Ordos Basin. *Minerals* **2023**, *13*, 314. https://doi.org/10.3390/min13030314

Received: 30 November 2022
Revised: 17 February 2023
Accepted: 20 February 2023
Published: 23 February 2023

Copyright: © 2023 by the authors. Licensee MDPI, Basel, Switzerland. This article is an open access article distributed under the terms and conditions of the Creative Commons Attribution (CC BY) license (https://creativecommons.org/licenses/by/4.0/).

1. Introduction

During the Middle Jurassic period, Eurasia became the largest landmass globally, while the North Chinese Platform and Siberian Platform constituted the main par, and its continental deposits were commonly developed (Figure 1a) [1,2]. The Jurassic was a typical greenhouse climate period when the carbon dioxide (CO_2) concentration was four times that of today, and the global average temperature was 5–10 °C higher than today [3–5].

Globally, although the temperature in the Jurassic was moderately higher, the climate varied distinctly at different times, with drastic fluctuations in temperature and humidity, accompanied by different geological events. For example, the Oceanic Anoxic Event with the maximum average temperature in the Early Toarcian [6–8]; the warming events during Early Bajocian, Middle Oxfordian, and long-term Late Jurassic [7,9,10]; and the cold intervals in the Late Pliensbachian and Late Callovian [11,12]. Similarly, the climate in different regions also had differences in the Jurassic, especially in northern China. In this area, the Hettangian–Pliensbachian was in a warm and humid climate, manifested in the extensive reproduction of ferns that liked the damp and heat [13]. During the Toarcian,

the temperature increased and was associated with a semi-humid and semi-arid climate. At this time, the heat-loving and dry-tolerant *Classopollis* pollen suddenly appeared in large quantities in the northern region [14], consistent with the warming event of the global terrestrial ecosystem [15]. The climate of the Aalenian–Bajocian returned to warm and humid and was dominated by abundant plants, such as *Ginkgoales, Czekanowskiales, Coniferales*, and *Filicinales*, and a certain number of coal-forming cycads [16,17], which provided the organic basis for multiple sets of thick coal seams widely occurring in the Yan'an Formation of the Ordos Basin, Xishanyao Formation of the Tuha Basin, and Dameigou Formation of the Qaidam Basin. The Bathonian–Callovian temperature increased again; this change is reflected in the large-scale distribution of red beds, the large changes in the fern spores content in warm and humid climates, and the increase in the heat-loving and dry-tolerant *Classopollis* pollen in continental basins in northern China. Moreover, the *Timiriasezvia-Darwinula arytirmenensis-Darwinula manna* assemblages, which reflect a brackish water environment, are found in the Toutunhe Formation in Xinjiang, Zhiluo Formation in Ordos Basin, Jiulongshan Formation in Northern Hebei, and Mawa Formation in Henan [17–19], indicating that the climate changed from warm and humid to semi-arid or arid conditions, and the high temperature and arid climate lasted until the end of the Jurassic [7,17,20]. Based on the analysis of paleoclimate change, floral record, spores and pollen assemblages, and regional stratigraphic correlation, the deposition age of the Zhiluo Formation coincided with the Bathonian–Callovian period, and the paleoclimate change was in a critical transition period from a warm and humid to a hot and arid climate [21–25].

Previous studies have shown that the Jurassic was a crucial period of tectonic stress field transformation, especially about 170 Ma ago, when the Yanshan Movement began to affect the Chinese continent, primarily during the transition from the closure of the Paleotethys tectonic domain to the circum-Pacific tectonic domain [26–28]. Zhao et al. (1996) experimented with the illite K–Ar dating and confirmed tectonic events in 160–170 Ma in the Ordos Basin [29]. Based on an analysis of thermal fluid records and detrital zircon age spectrum characteristics, Li et al. (2015) proposed that a strong tectonic activity appeared in the Ordos Basin around 168 Ma, which is consistent with the result that the basin's western margin experienced uplift at ±168.63 Ma according to the Zircon U–Pb dating and apatite fission track [30–32]. In terms of the stratigraphic contact relationship, the Zhiluo Formation displays an unconformity with the Yan'an Formation (Figure 1d) [32], correlating well with the Yanshan Movement episode I. The above proves that the Zhiluo Formation of the Middle Jurassic began to be deposited and was in a critical transformation period from the Paleotethys tectonic domain to the circum-Pacific tectonic domain. The transition time of the palaeotectonic domain was surprisingly consistent with that of the paleoclimate, and both changes occurred during the Zhiluo Formation's depositional period.

The geological study of the Zhiluo Formation in the Ordos Basin began in the 1970s and concentrated on the oil and gas discovery areas in this basin's western margin [33]. Recently, studying the Zhiluo Formation has attracted considerable attention from scholars due to the discovery of large uranium deposits (occurrences) in the basin's peripheral area [28,34–36].

Extensive studies have been conducted on the sedimentology of the Zhiluo Formation: Chinese scholars have analysed the types and distribution characteristics of sedimentary facies [36–40], stratigraphic sequence division [41,42], provenance analysis [37–39], and diagenesis [43]. They proposed corresponding sedimentary evolution models [24,37,38,42], or combined them with the regional geological structure [44,45] and highlighted their relationship with uranium mineralisation. However, the above research focused on the uranium-bearing ore areas and their vicinity around the basin, especially the sedimentology of the uranium-bearing reservoir in the lower sub-member of the Zhiluo Formation ($J_2Z^{1\text{-}1}$) [24,45,46]. Additionally, there are few studies on the sedimentology of the entire basin; only Zhao et al. (2007, 2008, 2010) preliminarily restored the sedimentary types and sand body distribution characteristics of the Zhiluo Formation in the entire region [47–49].

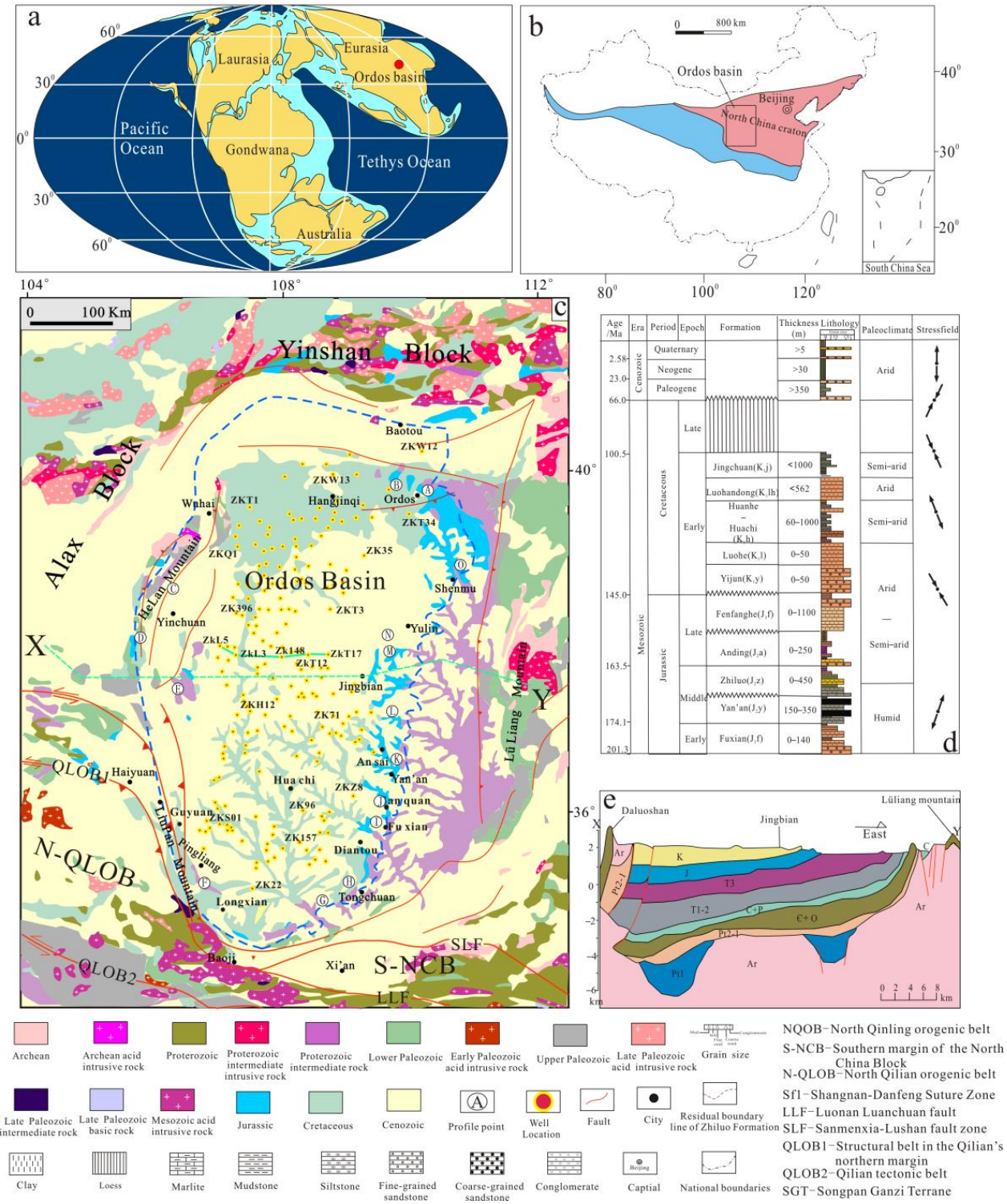


Figure 1. Location and geology maps of the Ordos Basin. (**a**) Middle Jurassic Bathonian (about 168 Ma) global Palaeogeographical map showing the position of Ordos Basin (modified after [50]). (**b**) The location of the Ordos Basin in China (modified after [51]). (**c**) Regional geological map of the Ordos Basin and its adjacent areas (modified after [52]). (**d**) Composite stratigraphic section of the Ordos Basin (modified after [53,54]). (**e**) East–West cross section XY of the Ordos Basin (modified after [55]).

The paleoclimate and tectonics jointly control the sedimentary system's depositional characteristics [17]. By analysing the existing sedimentary records, paleogeographic environment reconstruction can be achieved. However, studies on the Zhiluo Formation's depositional characteristics and sedimentary systems have often disregarded the paleoclimate conditions, severely restricting the understanding of the macroscopic and microscopic sedimentary changes of the Zhiluo Formation. Paleostructures are crucial in the sedimentary system change; however, research on the Zhiluo Formation's sedimentary filling evolution under the conditions of palaeotectonic transition has not been conducted effectively. Therefore, from the perspective of the entire basin, the Zhiluo Formation's sedimentary response characteristics and sedimentary filling evolution under the dual transition conditions of paleoclimate and paleostructure and the relationship between them (climate, tectonics and sedimentation) are discussed herein in detail. The main goal of this paper was to reconstruct the interplay between paleoclimate and paleotectonics, and guide sedimentological research in East Asia in light of the influence of tectonics and climate changes.

2. Geological Setting

Located in the western part of the North China Craton (NCC), the Ordos Basin is ranked the second largest sedimentary basin in China with an extension of ~2.5 × 10^5 km^2, and it contains abundant energy resources, such as oil, gas, coal and uranium-bearing deposits [32,56]. The current Ordos Basin presents a rectangular shape from north to south [57]. It is surrounded by the Yinshan and Qinling orogenic belts to the north and south, and the Helan–Liupan Mountains and Lüliang Mountain to the west and east, respectively [58,59] (Figure 1c).

The Ordos Basin is a large intracontinental basin formed on a basement of Achaean and Paleoproterozoic metamorphic rocks, Paleozoic neritic sedimentary rocks, and the cap rocks of Mesozoic–Cenozoic terrestrial sedimentary rocks [32,60], although Lower Carboniferous, Devonian and Silurian strata are absent [24]. Contrasted with the topography of the northwest higher and southeast lower, the Basin's strata show a gentle west-dipping monocline, with an angle of 1–5° [61,62]. Because of its tectonic location, the Ordos Basin is an unstable craton basin [63], affected by both the circum-Pacific tectonic domain in eastern China and the Paleotethys–Himalayan tectonic domain in Southwest China, and has the characteristics of a transitional zone of two tectonic domains, particularly since the Mesozoic [64,65]. In the Middle–Late Triassic, the Ordos Basin was compressed and uplifted among the Paleotethys oceanic crust to the southwest, the Alashan block to the northwest and the Yangtze plate to the southeast [66,67], and then developed into an independent large sedimentary basin. After this, the main geological tectonic framework of the basin was formed in the Yanshanian period and finally evolved into the present basin pattern (Figure 1e) [68,69].

From bottom to top, the Jurassic in the Ordos Basin was divided into the Fuxian, Yan'an, Zhiluo, Anding, and Fenfanghe Formations. The Zhiluo Formation was widely deposited and distributed over the Basin, and the strata thickness became thinner from west to east, with a thickness of 150–450 m and an average thickness of approximately 280 m (Figure S1). In terms of the stratigraphic contact relationship, the Zhiluo Formation unconformably lies on the underlying Yan'an Formation, and some areas are even directly in contact with the Yanchang Formation [49,70]. The top of the Zhiluo Formation is mainly in conformable contact with the overlying Anding Formation, but due to the uplifting and denudation in the later stage of the basin, the Zhiluo Formation in the basin's eastern margin presents an angular unconformity with the overlying Lower Cretaceous conglomerate [70,71].

3. Materials and Methods

3.1. Geological and Sedimentological Description

More than 15 outcrops from the Ordos Basin's margins, Well ZkS01 in the southwestern Basin, well ZkW12 in the Qingdamen area, and well ZkW12 in the Daying area in the north of the basin were described and measured (Figure 1c), including the Zhiluo Formation's rock colour, lithology, texture and sedimentary structures. Furthermore, the top-bottom boundary and contact relationship, strata thickness, palaeontological features and sedimentary facies were identified, analysed and classified, providing evidence for studying the sedimentary system, strata distribution characteristics and tectonic evolution of the Zhiluo Formation.

3.2. Thin Section Petrology

Thirty-nine thin sections were selected from outcrop samples in the Shenshangou, Gaotouyao and Zhongjizhen areas in the northern part of the basin, 150 thin sections were taken from outcrops in Zhenyuan County in the southwest of the basin, and 54 thin sections were obtained from outcrop samples in the Fuxian, Zichang, Yongshou and Linyou areas in the south of the basin. The Olympus TH4-200 optical microscope from the Cores and Samples Centre of Natural Resources was used to observe the thin sections in detail under crossed-polarised light and plane-polarised light systems at a magnification of 2×, 4×, 10× and 40× to identify the mineral composition of sandstone and make rock type statistics.

3.3. Lithofacies Palaeogeography Map

GR logging curves from 261 wells were used in the study area. Selected American petroleum institute units (80 API and above) were used as a baseline to distinguish mudstone and sandstone [72], and the contour lines were constructed at 10% intervals.

4. Results

4.1. Petrological Characteristics

The Zhiluo Formation can be divided into an upper member (J_2Z^2) and lower member (J_2Z^1) (Figure 2), and the lower member is further divided into the upper sub-member ($J_2Z^{1\text{-}2}$) and lower sub-member ($J_2Z^{1\text{-}1}$) [73,74]. Its sedimentary characteristics are as follows.

(1) The lower part of $J_2z^{1\text{-}1}$ primarily comprises grey, yellow-green, greyish-green coarse sandstone and medium sandstone, with large-scale trough cross-bedding and tabular cross-bedding (Figure 3a). Conglomerate and conglomeratic sandstone are typical at the bottom of $J_2z^{1\text{-}1}$, with an evident channel scouring surface. The upper part of $J_2z^{1\text{-}1}$ comprises greyish-green and greyish-white medium-fine sandstone, intercalated with thin coal lenses or seams in the northeast of the basin (Figure 2a), and with a thin greyish-black mudstone or siltstone layer, and shows small-scale cross-parallel and horizontal beddings in other areas of the basin. The strata become finer upwards with rich medium-coarse and gravel-bearing sandstone. Reducing substances, such as plant remains, carbonaceous debris and pyrite, are found in the sand bodies (Figure 3b,c), and most pyrites occur in lump shape (Figure 4a). The sandstone of the strata primarily shows clast-supported textures in point-line contact and poor sorting and roundness (Figure 4b). Ferruginous cements are common in the formation's sandstone.

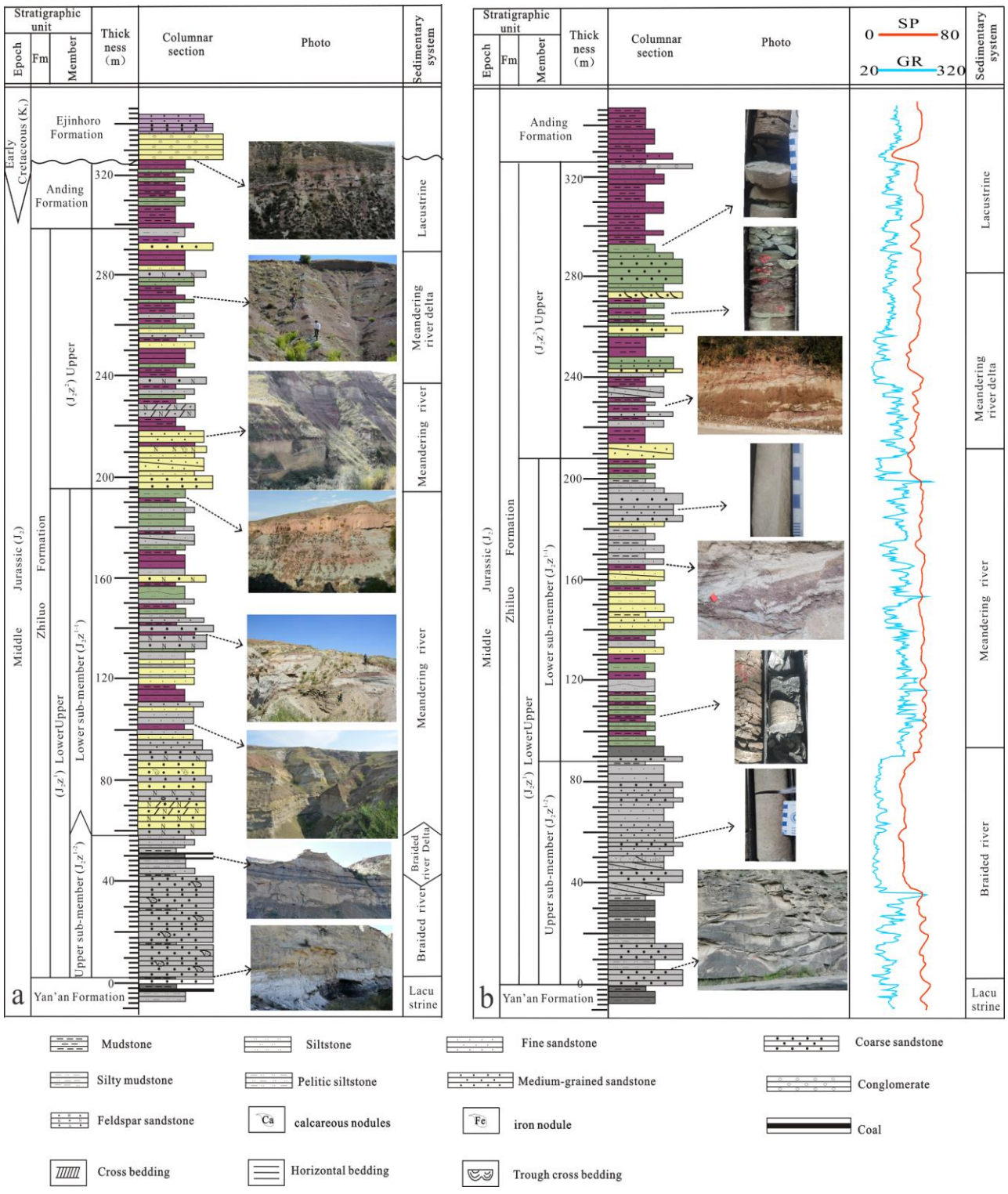


Figure 2. (**a**) Composite stratigraphic section of the Jurassic Zhiluo Formation in the basin's northern part (modified from Shenshangou section Ⓐ and Gaotouyao section Ⓑ; see Figure 1c); (**b**) Composite stratigraphic section of the Jurassic Zhiluo Formation in the basin's southern part.

(2) The lower part of $J_2z^{1\text{-}2}$ comprises light greyish-green and light-yellow medium and fine sandstone, with medium-scale crossbedding. The upper part of $J_2z^{1\text{-}2}$ primarily contains greyish-yellow, greyish-green, brown and dark purple siltstone and mudstone, characterised by a thin interbedding of medium-fine sandstone, siltstone and

argillaceous rock and shows horizontal bedding, small cross-bedding, and climbing-ripple cross-lamination (Figure 3d,e). Plant remains and carbonaceous debris in the sand body are markedly reduced. The sedimentary structure is characterised by coarse grains in the lower layer and fine grains in the upper layer, with an evident fining upward trend. The grains are sub-angular to sub-rounded but have good sorting. There are muddy matrix and calcareous cements (Figure 4c) and some ferruginous cements.



Figure 3. Sedimentary structures and lithologic characteristics of the Zhiluo Formation. (**a**) Trough and tabular crossbeddings, Zhiluotown section. (**b**) Plant remains and carbonaceous debris, Shenshangou section. (**c**) Pyrite nodule, Hengshan area. (**d**) Horizontal bedding, climbing-ripple cross-lamination, Zhiluotown section. (**e**) Small crossbedding and horizontal bedding, Zhongjitown area. (**f**) Small-scale crossbedding, Shenshangou section. (**g**) Brownish red fine sandstone and siltstone with small-scale crossbedding and horizontal bedding, Zhongjitown area. (**h**) Medium-coarse-grained braided channel sandstone, obvious channel scouring surface at the bottom of the sandstone, Zhiluotown section. (**i**) Delta front subfacies, Ansai section. The arrow in the images shows the position of the phenomena.

(3) The lower part of J_2z^2 is grey, khaki medium-fine sandstone, with medium-large troughs and tabular cross-bedding. The lithology changes upwards into khaki fine sandstone and variegated (brown-red, purple-red and purple-brown) siltstone and mudstone, intercalated with thin layers of greyish-green and purple-red medium-fine sandstone and siltstone, and shows small-scale crossbedding and horizontal bedding (Figure 3f,g). The strata are characterised by the thin interbedding of sandstone and mudstone in repeated fining upward cycles. Secondary gypsum veins and ferritisation are found and distributed along the fractures in a patchy or banded pattern in the upper layer of this formation (Figure 4d,e). The grains are typically identified as sub-angular to sub-rounded, with good sorting. The cements are primarily calcareous and ferric (Figure 4f).

Quantitative statistics of the sandstone thin sections of the Zhiluo Formation in the periphery of the Ordos Basin reveal that the rock types in the north of the basin are mainly feldspathic lithic sandstone and lithic feldspar sandstone, followed by lithic sandstone, feldspathic quartz sandstone, arkose and a small amount of quartz sandstone (Figure 4g). The sandstone in the western margin is composed of arkose and lithic sandstone [39,42] and is dominated in the southwest by lithic quartz sandstone and feldspathic lithic sandstone (Figure 4h). The rock types in the south of the basin are mainly arkose sandstone or feldspathic quartz sandstone (Figure 4i).

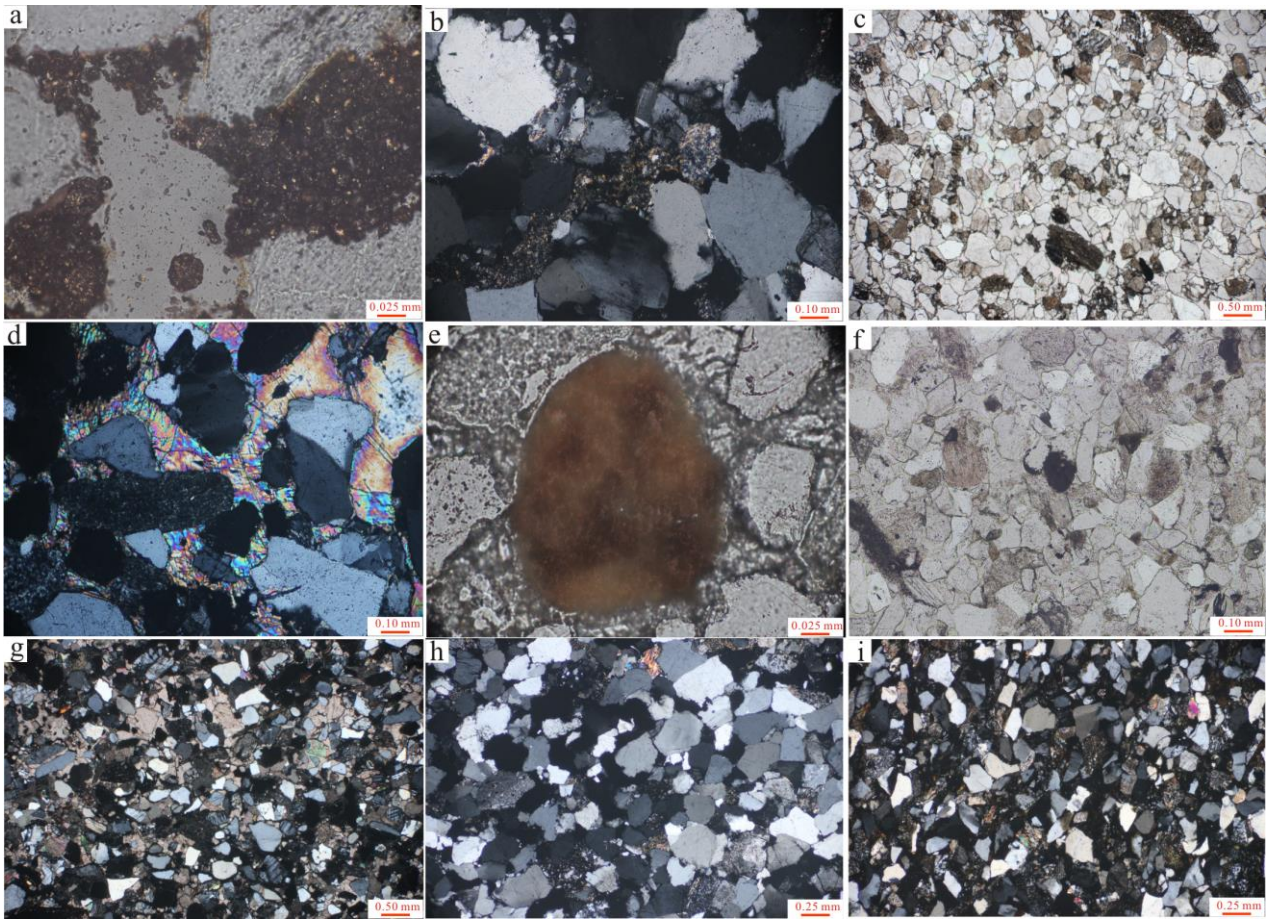


Figure 4. Representative photomicrographs of Zhiluo Formation Sandstone. (**a**) From well ZkS01 at 1938.6 m, light yellowish white pyrite, plane-polarised light 40×. (**b**) From well ZkS01 at 1933.3 m, line–point contact, crossed-polarised light, 10×. (**c**) $J_2z^{1\text{-}2}$, Linyou area, chlorite and calcareous cement, plane-polarised light, 2×. (**d**) J_2z^2, Linyou area, secondary gypsum, crossed-polarised light, 10×. (**e**) J_2z^2, Linyou area, limonite, reflected light, 40×. (**f**) From well ZkS01 at 1715.2 m, chlorite and calcareous and iron cements, plane-polarised light, 10×. (**g**) $J_2z^{1\text{-}2}$, Shenshangou area, feldspar sandstone, crossed-polarised light, 2×. (**h**) From well ZkS01 at 1928.6 m, quartz sandstone, crossed-polarised light, 4×. (**i**) $J_2z^{1\text{-}1}$, Fuxian area, feldspar sandstone, crossed-polarised light, 4×.

4.2. Palaeontological Record

There are relatively few fossil types in the Jurassic Zhiluo Formation, primarily in the lower strata, while the fossils found in the upper strata are mostly distributed in the southeast of the basin.

In the Zhiluo Formation's lower part, plant fossils typically occur throughout the basin, including silicified wood of higher plants, plant stem debris, relatively intact fossil stems and leaves, and underoxidised plant remains and carbonaceous debris (Figure 3a). The plant types of the Zhiluo Formation are mainly ferns (mean values 62.75%) and gym-

nosperms (mean values 37.25%). Therefore, *Cyathidites* are the most prosperous (40.83%), followed by *Osmundacidites* (13.92%), a certain amount of *Disacciatrileti* (18.37%), *Cycadopites* and *Chasmatosporites* (11.21%), *Classopollis* (3.66%), *Callialasporites* and *Cerebropollenites* (2.36%), and other types of sporopollen [22]. The *Classopollis* content in the Lingwu area in the basin's western part is up to 28.81% [25]. In the basin's east and northeast, fossils are abundant, mainly ferns and Ginkgoinae, but the content of gymnosperms is significantly lower than that of the Yan'an Formation. Among these fossils, *Cyatheaceae*, *Coniferae*, and *Cycadaceae* occur the most, and the *Cheirolepidiaceae* and *Araucariaceae* contents are remarkably increased compared with that of the Yan'an Formation [22,24,38]. Fern spores and gymposerm pollen can be found in the Fuxian area in the basin's south [47].

In the Zhiluo Formation's upper part, fossils are rare. Among them, plant root fossils are occasionally seen in the basin's northeast. Animal fossils, such as bivalves, conchostraca, sporadic fish scales and some incomplete plant fossils, are occasionally found in the mudstone in the Jingbian–Fuxian area [47,48,75], and a small amount of spores and pollen and bivalve fossils occur in the basin's western margin [39].

4.3. Lithofacies Palaeogeography and Provenance

Within the study area, 261 wells' log data and 15 outcrops were selected for comparison in the Zhiluo Formation, and the contour lines were drawn at 10% intervals. In addition to paleocurrent field measurements, the authors used the results of previous provenance analysis on the northern, western and southern parts of the Zhiluo Formation in the basin. The basin's provenance primarily originates from the ancient metamorphic and magmatic rocks in the Langshan–Wulashan–Daqingshan area to the north, the intermediate-acid magmatic and metamorphic rocks in the Alxa block to the northwest [23,46,61,73], the intermediate-acidic, basic magmatic and metamorphic rocks in the Qilian Mountains to the southwest, the Qinling Mountains to the south, and the clastic rocks in the southern margin of the North China Block to the south (Figure 1c) [23,36,76].

4.4. Sedimentary Facies Characteristics

Braided river facies. The lithology of braided river facies is mainly composed of grey, yellow-green and greyish-green medium-coarse and medium-fine sandstone. The top of the braided river shows greyish-green, grey-black siltstone and mudstone, and the local area at the bottom is a thin layer of conglomerate or gravel-bearing sandstone. The gravel-bearing sandstone is characterised by fine gravel sandstone and medium-coarse sandstone development. Braided river facies has a typical fining-upwards sedimentary sequence of sandstone-wrapped mudstone. Field outcrop measurements show that the channel sand bodies of the braided river have a large width/thickness ratio (Figure 2b). The logging curve presents a thick-bedded box or combined box-bell shape, and a high-amplitude box shape with an extremely thin finger shape dominates the natural GR log (Figure 5).

Braided river delta facies. Several subfacies are identified in braided river delta facies. The braided river delta plain subfacies' medium-coarse sandstone mainly consists of grey, greyish-yellow and blue-grey, with small to medium-sized tabular and trough cross-bedding. Silicified wood and much carbonaceous debris can be seen in local sand bodies. Siltstone and argillaceous siltstone are developed in the upper part of medium-coarse-grained sandstone, with horizontal bedding and fine-grained sediments. The spontaneous potential (SP) curve shows a low amplitude zigzag shape, interpreted as an interdistributary bay. A small crossbedding with a thin layer of fine lenticular sandstone is found in the mudstone and argillaceous siltstone, representing crevasse splay.

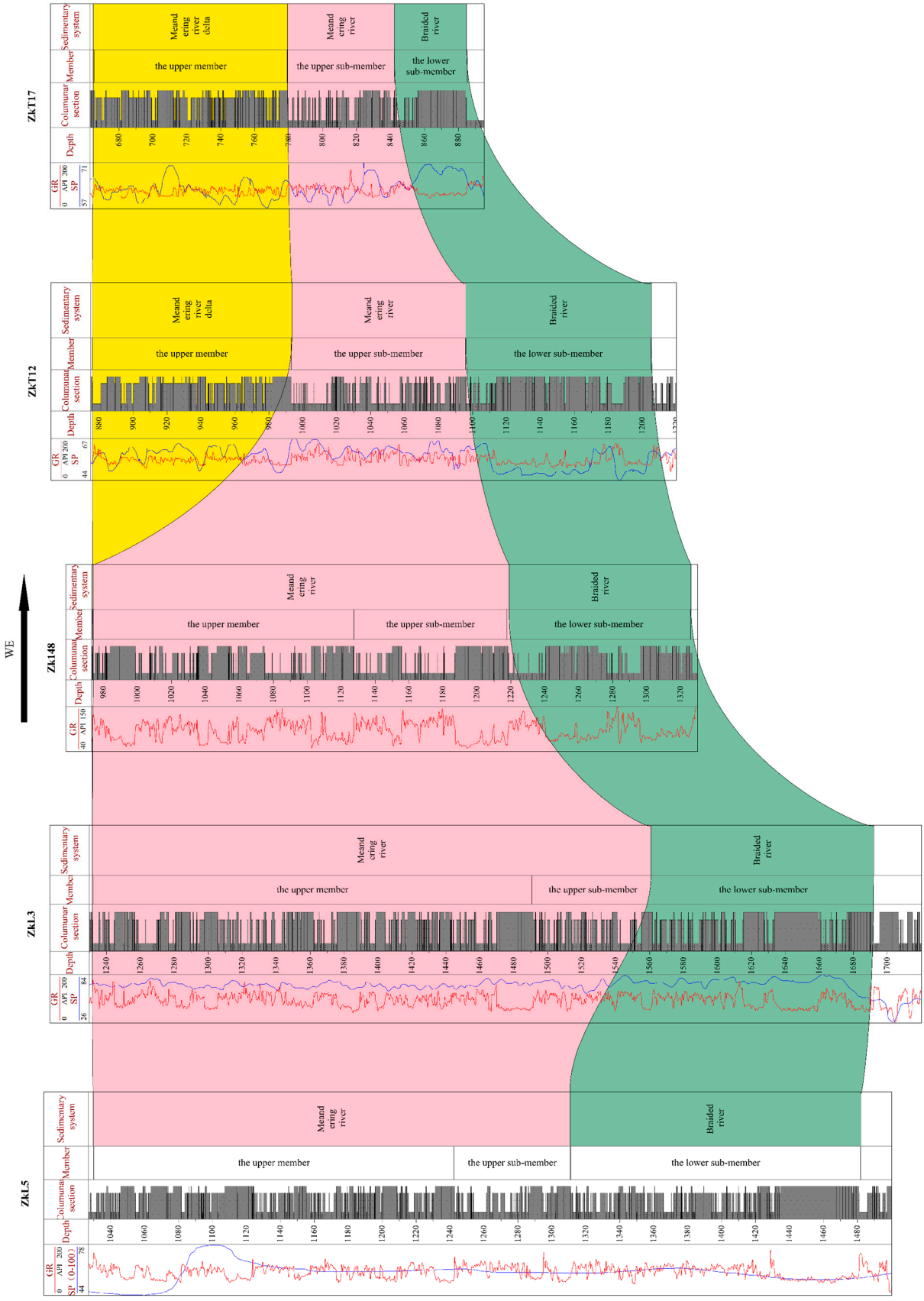


Figure 5. Well-correlation section of the Jurassic Zhiluo Formation in the basin's Middle part from west to east.

Meandering river facies. The meandering river sedimentary facies is further divided into channel floor lag, point bar, embankment and overbank subfacies. The channel floor lag was deposited in the lower part of the meandering river sedimentary facies and comprises grey, greyish-green, light-yellow gravel, gravel-bearing coarse sandstone and coarse sandstone. The channel floor lag is thin and has a lens-shaped distribution, with a lack of bedding structure inside and a visible scouring phenomenon at the bottom. The grain size of the channel floor lag becomes finer upward, and the GR curve displays a combined box shape to an abrupt zigzag shape at the bottom (Figure 5). The point bar primarily comprises greyish-yellow, khaki, greyish-green and greyish-white medium-fine sandstone, locally mixed with gravelly sandstone and siltstone. The sand bodies have a wide range of grain size variations. As the grain size of the sand bodies becomes finer upward in this interval, the bedding scale becomes smaller, from medium-large trough and tabular crossbedding (Figure 3d) to small trough crossbedding, tabular crossbedding and horizontal bedding (Figure 3e). Trunk fossils, plant debris and carbonaceous debris can be found in the strata. On the logging curve, SP and GR curves show the characteristics of a bell-zigzag shape combination with a similar thickness. The embankment subfacies are greyish-green, grey, purple-red siltstone and fine sandstone interbedded with thin layers of greyish-green and dark purple mudstone, with cross-bedding, horizontal and small oblique beddings. This presents multi-stage depositional cycles of interbedded sandstone and mudstone with unequal thickness. The lithology of the overbank at the top of the meandering river facies is composed of greyish-green, purple, and purple-red mudstone and siltstone, with various small cross-bedding, climbing ripple, and horizontal and oblique beddings.

Meandering river delta facies. The meandering river delta facies can be divided into delta plain and delta front subfacies. The lower part of the delta plain subfacies is primarily yellow-grey medium-fine sandstone, with medium trough crossbedding and a clear scouring surface at the bottom, reflecting the distributary channel characteristics. Purple-red, greyish-green mudstone, silty mudstone and argillaceous siltstone occur on the distributary channel and are interbedded and widespread across the area. Its logging curve presents a zigzag shape, with high GR and high resistance, displaying the sedimentary characteristics of interdistributary bay microfacies. The delta front subfacies consist of purple-red, greyish-green mudstone, silty mudstone and siltstone intercalated with thin layers of fine sandstone. Small oblique beddings can be seen in the fine sand body, showing the sedimentary characteristics of an underwater distributary channel.

Lacustrine facies. The lacustrine facies of the Zhiluo Formation is mainly composed of variegated mudstone and siltstone, such as greyish-green, purple-red, brown-red, greyish-yellow and blue-grey, and (or) is intercalated with medium-thin layers of grey, greyish-green and purple-red fine sandstone. The sandstone has good sorting and roundness. The lacustrine facies is divided into shore and shallow lacustrine subfacies (Figure 2b). The shore lacustrine subfacies comprise a medium-thin layer of siltstone and fine sandstone intercalated with mudstone, with wavy ripple bedding, tabular crossbedding and ripple mark bedding, and worm traces, bivalves, ostracods and other fossils can occasionally be observed [47,75]. The shallow lacustrine subfacies are dominated by greyish-black and greyish-green mudstone and interbedded variegated mudstone and siltstone with horizontal or small wavy bedding, and animal fossils can be seen in the strata [47,48].

5. Discussion

5.1. Sedimentary System

Elemental geochemistry is an effective method for paleoclimate discrimination, and indices such as Sr, Rb/Sr, Sr/Cu, Sr/Ba, and Al_2O_3/MgO ratios are good for discriminating paleoclimates (Table S1) [77–79].

Low content of Sr indicates a warm and humid climate, while high content indicates a dry and hot climate; the Sr/Cu ratio between 1.3 and 5.0 indicates a warm and humid climate, and a ratio higher than 5.0 indicates a dry and hot climate [80]. The Rb content is relatively stable in chemical weathering, while the Sr content is easy to change. Therefore, in a humid climate, due to more precipitation and strong weathering, the Sr is easy to be washed away, resulting in a higher Rb/Sr ratio. On the contrary, in an arid climate, the Rb/Sr ratio is relatively low [23,81]. The Sr/Ba ratio is a sensitive indicator for paleosalinity analysis, and keeps a significant positive correlation; when the Sr/Ba ratio is less than 0.5, it indicates a freshwater environment, while a Sr/Ba ratio between 0.5 and 1.0 indicates a brackish water environment [21,81]. The Al_2O_3/MgO ratio can also indicate the paleoclimate change. The higher the ratio, the more desalinated the water during the deposition period, indicating a warm and humid climate. On the contrary, the smaller the ratio, the more arid the climate [79].

Based on drilling cores, logging data and field outcrops combined with rock assemblage characteristics, palaeontological characteristics, sedimentary facies markers, and comprehensive previous research results [36,42,47], the sedimentary facies and environment of the Zhiluo Formation in the Ordos Basin can be identified and analysed (Figures 2 and 5).

5.1.1. Braided River–Braided River Delta Depositional System

The mudstone's Sr content is low and the average value is 150.67 × 10^{-6} ωB/μg·g^{-1}, the Sr/Cu value is less than 10 and the average value is 6.19, and the average Rb/Sr ratio value is relatively high (0.65) [21]. In addition, Song et al. (2020) found that the Rb/Sr ratio of the Zhiluo Formation's mudstone in the Lingwu area in the basin's western sector is also relatively high and the average value is 0.73, illustrating a warm and humid climate [25]. Coal is an indicator of a humid climate, and the occurrence of coal seams or coal lines in the strata in the basin's northeast and west further indicates the warm and humid climate in this period (Figures 2a and S1). The Sr/Ba ratios are less than 0.5, with an average value of 0.19, and the Al_2O_3/MgO value is large, indicating that the sediment deposition was typically under the condition of a freshwater environment (Figure 6). Therefore, the depositional system was mainly formed under the warm and humid climate during the $J_2z^{1\text{-}1}$ sedimentary period.

(a) Braided river facies. Braided river facies are widely developed in the entire area. Taking the Qingcheng–Huangling area as the dividing line, the strata thickness of braided river facies in the basin's north becomes thinner from northwest to southeast and north to south, whereas the thickness in the basin's south gradually thins from southwest to northeast.

During this sedimentary period, the thickness of braided channel sand bodies was large, and the lateral distribution was relatively stable due to heavy rainfall and sediment supply. From the base upward, the grain size tends to become finer upwards. A clear channel scouring surface occurs at the bottom of the sandstone (Figure 3h), with medium-large trough and tabular crossbedding upward, transitioning to small-medium crossbedding and parallel bedding, indicating a sedimentary process with a gradual weakening of the water flow energy. The warm and humid climate is conducive to organic matter production. Therefore, plant remains are common in the entire region, showing a high-energy traction flow sedimentation. The spore and pollen fossil assemblages in the Zhiluo Formation are similar to those in the Yan'an Formation, with ferns, Ginkgoinae and gymnosperms in the majority, which is a continuation of plant types under warm and humid climates [22]. Additionally, there are also more reducing substances, such as carbonaceous debris and pyrite in the strata, indicating that it was in a reduction environment rich in organic matter.

It is speculated that the precipitation was large, the water level was high at that time, and the braided river sediments remained below the water surface for a long time.

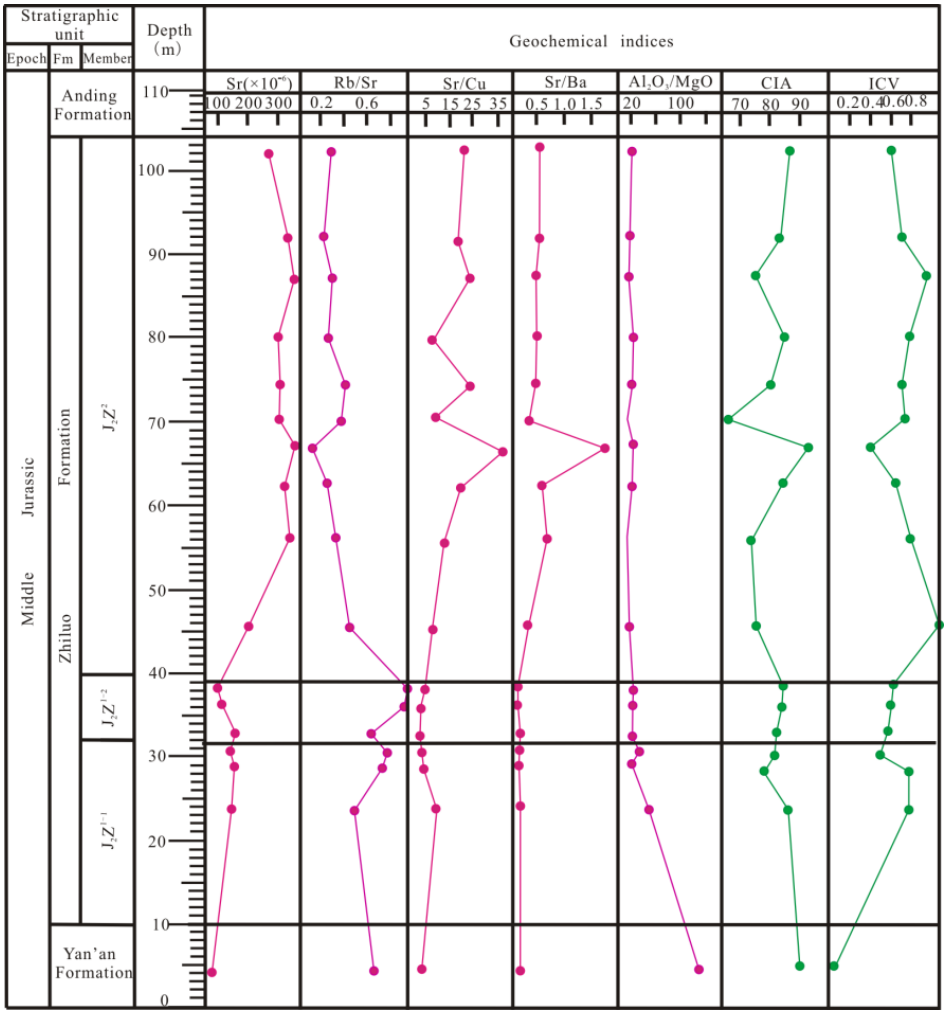


Figure 6. The vertical variation map of the geochemical parameters of Jurassic Zhiluo Formation mudstones in the Shenshangou area of Ordos Basin (modified after [21,22]).

(b) Braided river delta facies. Influenced by the east-west fault structural belt of Sunjialiang–Zaohuohao [82], the terrain in the south of this structural belt becomes flat, and the number of branch channels of the braided river and the mudstone content gradually increase, transforming the braided river in the basin's north into the braided river delta plain; regionally, the braided river delta plain is mainly distributed in the vast area south of the Yijinhuoluo –Shenshangou line in the basin's northeast [43,74].

The channel scouring surface at the bottom of the braided river delta plain is exposed, showing the sedimentary characteristics of the braided river delta distributary channels. Siltstone and argillaceous siltstone are developed in the upper part of medium-coarse-grained sandstone, with horizontal bedding and fine-grained sediments with lake characteristics [35,74]. Vertically, the crevasse splay and interdistributary bay in the lower part present characteristics of a coarsening-upward sequence [73]. Several sets of thin lenses or seams occur in the strata (Figure 2a), reflecting that the coal-bearing strata were formed in the warm and humid overbank swamp environment during this period. The braided river delta's sand bodies are distributed horizontally in a bird foot shape, indicating that the depositional centre of the braided river delta was located in its southeast direction.

Compared with J_2z^{1-1}, the small-scale braided rivers in J_2z^{1-2} were formed in the Piedmont area of the basin margin in the north of the Yinchuan–Etuokeqi–Dongsheng

area and in the south of the Pengyang–Qingcheng–Huangling area; material sources of sediment area was caused by seasonal flooding. Although their lithological and structural characteristics are similar to those of J_2z^{1-1}, the lateral continuity of the braided channel sand bodies becomes worse, and the channel diversion is more frequent. As the climate became drier, resulting in less rainfall and lower water levels, the sediments were more exposed, and the reducing substances, such as plant debris and pyrite, were significantly reduced.

5.1.2. Meandering River–Meandering River Delta Depositional System

(a) Compared with J_2z^{1-1}, the Sr content increases and the average value is 305.6 × 10^{-6} $\omega_{B/}\mu g{\cdot}g^{-1}$, the Al_2O_3/MgO ratio decreases and the average value is 7.55 [21], the Sr/Ba ratio is basically close, with an average value of 0.18, testifying that although the climate changed to semi-arid, the water conditions still belonged to a freshwater environment (Figure 6). Among the fossil pollen, Cycadaceae and Coniferae were abundant in the period; furthermore, the Cheirolepidiaceae and Araucariaceae content increased remarkably, correlating with the semi-humid and semi-arid climate [22,38]. Thus, during the sedimentary period of J_2z^{1-2}, the climate gradually transited from warm and humid to semi-humid and semi-arid, the sediment supply weakened and the region was characterised by the development of low-sinuosity meandering rivers.

Although the climate became arid, some rainfall still occurred, and grey tones dominated the colour of the rocks in the meandering river sedimentary facies' lower part. Trunk fossils and plant debris are significantly reduced, showing that the climate gradually became arid from the perspective of oxidative decomposition, increasing the degree of oxidation, which is inconducive to preserving organic matter. As the grain size of the sand bodies becomes finer upward, the bedding scale becomes smaller from large-medium bedding to small crossbedding (Figure 3e); this indicates that the hydrodynamic conditions tend to weaken from the bottom up.

The overbank is the product of the low-lying areas with weak hydrodynamic conditions, formed when the river overflowed the riverbed during the flood period. The purple and purple-red tone rocks in the embankment and overbank significantly increased, which was related to the indirect exposure of sediments to the surface and the temperature increase and significant climate characteristics of alternating dry and wet in the entire area, increasing Fe^{3+} in the rocks, which is also concordant with the lower content of pyrite in the strata.

(b) In this period, compared with J_2z^{1-2}, the average content of Sr is higher, with an average value of 408.67 × 10^{-6} $\omega_{B/}\mu g{\cdot}g^{-1}$ [21]; Lei et al. (2017) found that the average Sr value of J_2z^2 (311.2) was significantly higher than that of J_2z^1 (137.8) [23]. The Sr/Cu value is higher than 10 and the average value is 19 [21]. The measured value average of J_2z^2 (14.51) is higher than that of J_2z^1 (8.10) in the Hangjinqi area [23]. The Rb/Sr value decreases significantly, with an average value of 0.31; Song et al. (2020) found that the Rb/Sr ratio of the Zhiluo Formation in the Lingwu area in the basin's western sector ranged from 0.50 to 0.82, decreasing vertically [25]. The average Sr/Ba ratio value of J_2z^2 (0.68) is almost 3.5 times that of J_2z^1 (0.19) [21], indicating that under the hot and arid climate, evaporation increases and the water environment is brackish (Figure 6). Thereby, during the depositional period of J_2z^2, the temperature in the entire region further increased, the climate became more arid, the supply of sediment sources was insufficient, and the meandering river presented high sinuosity of sedimentary characteristics. The meandering river delta was developed in the transition area between the lake and land; however, the meandering river's sedimentation was prominent because of the lake's weaker hydrodynamic conditions.

Compared with J_2z^{1-2}, the cycles from coarse to fine in this period are repeated more frequently, and the meandering river facies is characterised by a thin lower layer and a thick upper layer, with a more measurable binary structure.

The grain size of the sediments in this period is finer in this interval; only a small amount of plant and carbonaceous debris remains in the strata, and the frequency of

lateral erosion, migration and accretion of the meandering channel's sand bodies are more common. Due to seasonal flooding, it is easy for water flow to break through the river channel and form embankment and overbank deposits. The overbank subfacies are widely distributed, and the strata are relatively thick. Limonite commonly occurs in this interval, as the product of an arid oxidation environment. Fossils and sporopollenin are scarce in the Zhiluo Formation's upper strata, reflecting that the hot and arid conditions are unfavourable to plant growth and preservation.

The meandering river delta facies are mainly distributed in the south of the Yijinhuoluo–Dongsheng area to the Shenmu area in the northeast of the basin, the Jingbian–Zhidan–Wuqi–Huanxian area in the central part of the basin, and the Zhenyuan–Zhengning area in the south of the basin. The delta plain and front can be identified through field outcrops and drilling cores (Figure 3i).

The grain size probability cumulative curve of sand bodies in the delta plain subfacies shows a three-segment shape with a small slope, highlighting that the sediments are formed under traction flow conditions [47,83]. The sediments in the delta front subfacies present a vertically coarsening-upward sequence, showing characteristics of interbed development between underwater distributary channels and silty mudstone-dominated interdistributary bays. During this period, the delta's development area was small, affected by the meandering river's flow. The coarse-grained rocks in the strata are grey and yellow-toned, whereas the fine-grained and mud-grained rocks are purple and purple-red-toned, demonstrating that in the water-land transition area of a hot and arid climate, red-toned sediments are easily promoted.

5.1.3. Lacustrine Depositional System

Lacustrine facies are distributed in the upper part of J_2z^2 and belong to the brackish-water lake environment. Shore-shallow lacustrine subfacies can be identified in the residual basin; in the Shenmu area to the northeast, the Hengshan area to the middle and east and the Huachi–Fuxian–Ansai area to the south.

In the upper layers of the lacustrine facies, secondary gypsum veins and ferritisation are found and distributed along the fractures in a patchy or banded pattern (Figure 4d,e), indicating a significant arid–semi-arid climate. Several mud cracks were preserved at the top of the Zhiluo Formation in the basin's southeast, reflecting the further intensification of the evolution towards drought climates [47]. The small trough crossbedding, tabular crossbedding and ripple mark bedding in the shore lacustrine subfacies reflect the combined action of currents and waves from the lake basin. Worm traces, bivalves, ostracods and other fossils can be found, indicating the characteristics of shore-zone sediments with moderately active hydrodynamic conditions [47,75]. The shallow lacustrine subfacies are dominated by greyish-black and greyish-green mudstone and interbedded variegated mudstone and siltstone. The cyclic sedimentation is caused by seasonal flooding. Additionally, animal fossils, such as bivalves and fish scales and a small number of plant fossils, can be seen [47,48], showing a quiet lacustrine shallow water environment.

As the Zhiluo Formation's paleoclimate in the basin changed from warm and humid in the early stage to hot and arid in the middle and late stages [21,22,24,25], the strata present different sedimentary features (Figure 7). From the above-mentioned stratigraphic distribution of the Zhiluo Formation in the basin, the differentiation characteristics of clear sedimentary facies occur both vertically and horizontally. The early sedimentary stage of the Zhiluo Formation mainly developed the braided river. In the middle sedimentary stage, the western mountain margin area was still characterised by braided river facies, whereas the other areas deposited low sinuous meandering river facies. In the late sedimentary stage, the west distributed high sinuous meandering river facies, the middle developed delta facies, and the southeast evolved into lacustrine facies.

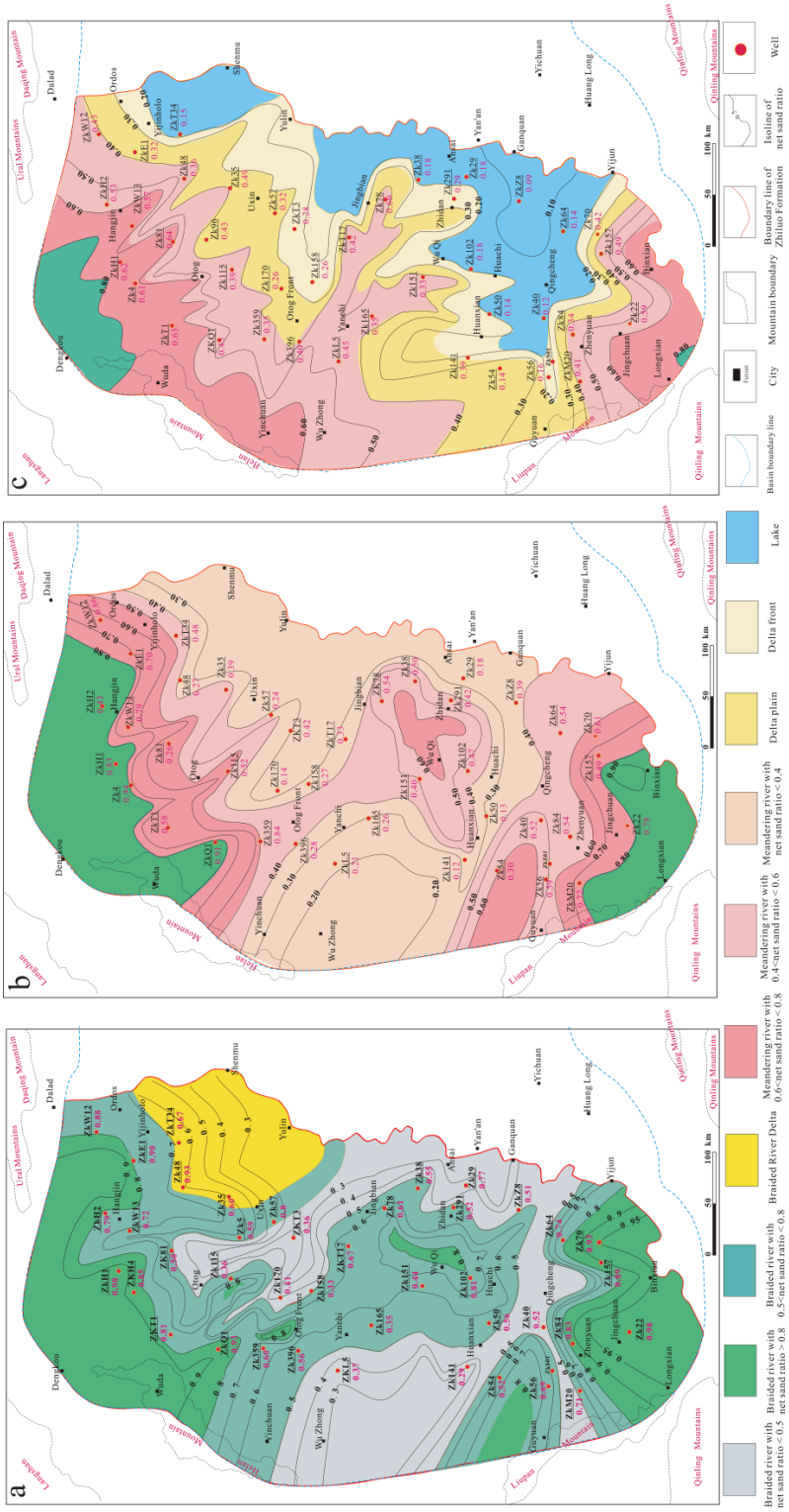


Figure 7. Lithofacies paleogeographic map of the Jurassic Zhiluo Formation. (**a**) Lithofacies paleogeographic map of the $J_2z^{1\text{-}1}$; (**b**) Lithofacies paleogeographic map of the $J_2z^{1\text{-}2}$; (**c**) Lithofacies paleogeographic map of the J_2z^2.

5.2. Sedimentary Filling Evolution

The uplift of the Yanshan Movement episode I affected the Ordos Basin, which broke the previously unified Great North China Basin, raised the northern and eastern margins of the Ordos Basin, and shrunk the lakes, and the sedimentary system transformed the

lake delta in the late Yan'an Formation to the braided river deposition of the Zhiluo Formation [32,42,84].

During the deposition period of the Zhiluo Formation, the eastern boundary of the Ordos Basin moved westward to the west of the Taihang Mountains [48]. After a brief uplift and denudation corresponding to the upper part of Yan'an Formation, the Ordos Basin subsided and began to be filled by sediments. At this time, the climate in most parts of China changed, which manifested in the transition from warm and humid to hot and arid [85].

During the J_2z^{1-1} deposition period, the basin subsided stably, and the overall landform was high in the north and low in the south. The depocentre is located southeast of the residual basin. Because the study area was in a warm and humid environment in northern China, plants were very prosperous, mainly ferns, Ginkgoinae and gymnosperms. In this period, the elevation difference between the sedimentary area and its periphery was large, resulting in strong hydrodynamic conditions in the provenance area and a sufficient supply of sedimentary materials. The Yinshan Mountain to the north and the Alxa block to the northwest of the basin maintained a large slope angle with the surface in the basin, making the provenance supply rich and easy to form a large-scale, long-distance sediment transport slope area. The developed braided river sand bodies were thick, overlapping, and accumulated with each other vertically and extended horizontally in the NE and NS directions. The river channels were intertwined into a grid-like distribution, an important transport corridor for the sediments.

The clastic sediment transport channel in the northeast of the basin is closely related to the activities of the east-west fault tectonic belt of the Sunjialiang–Zaohuohao area [82]. The terrain in the south of this structural belt becomes flat, and the number of branch channels of the braided river increases, promoting the transition of sedimentary facies from the braided river to the braided river delta [43,74]. The clastic material's dispersal direction is perpendicular to the strike of the above-mentioned structural belt, and it is distributed in a bird's foot shape. The vegetation in this period was lush, providing the material for coal formation. Compared with the provenance in the basin's north, the short-distance sediment supply in the Qilian–Qinling orogenic belt and the southern margin of the North China block in the basin's south were weak and transported clastic sediments in the SW–NE direction. Although the dispersion range of the channel sand bodies is small, the thickness is still large; they overlapped with each other, distributed in a network and finally converged in the Qingcheng–Fuxian area (Figure 8a).

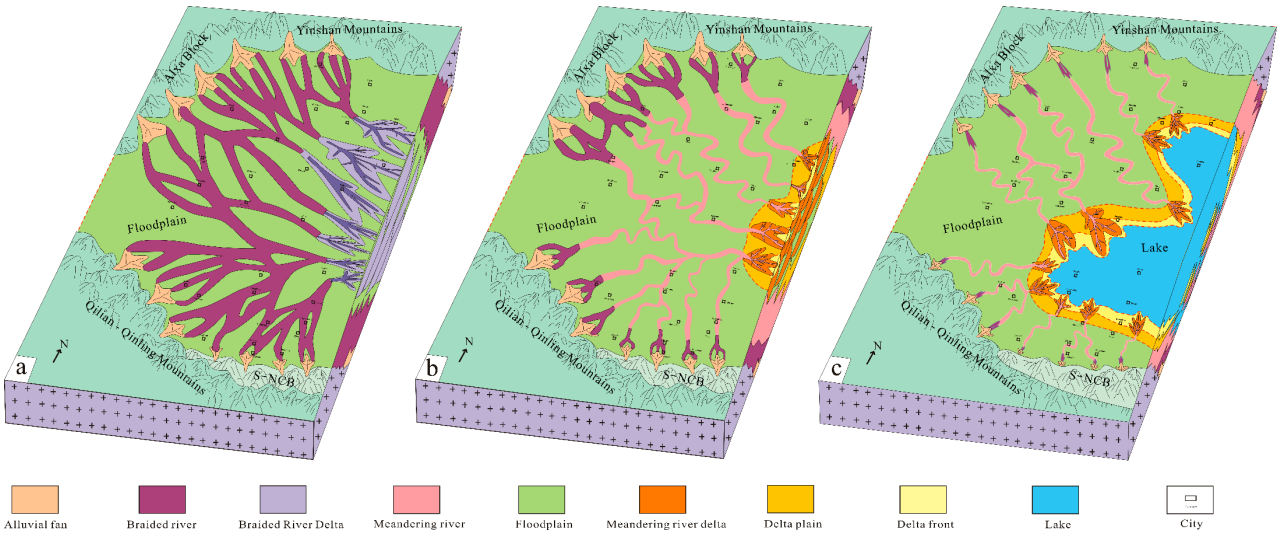


Figure 8. Sedimentary filling evolution map of Jurassic Zhiluo Formation in Ordos Basin: (**a**) Sedimentary filling evolution map of the J_2z^{1-1}; (**b**) Sedimentary filling evolution map of the J_2z^{1-2}; (**c**) Sedimentary filling evolution map of the J_2z^2.

During the J_2z^{1-2} depositional period, the tectonic stress of the Yanshan Movement episode I became weaker. The basin's western margin presented a slight east-trending overthrust, and the basin's eastern part was slowly uplifted. The main body of the basin rose slowly, and the boundary gradually shrank westward. The climate was changing to a semi-humid and semi-arid environment, changing plant types and increasing ferns, Cycadaceae, Coniferae, and a certain amount of Bennettitales and Ginkgoinae. Compared with the J_2z^{1-1} period, the basin's paleotopographic height difference decreased, the hydrodynamic force weakened, and the supply of clastic sediments decreased. The depocentre migrated towards the basin's northwest but was still distributed in the southeastern part of the basin. In the Piedmont area around the basin, braided rivers were still deposited, but meandering rivers gradually occurred in the middle of the basin. Under the joint action of the long-distance provenance in the basin's north and the short-distance provenance in the south, the clastic materials were transported into the basin (Figure 8b).

The J_2z^2 sedimentary stage was in the tectonic transformation period of the Yanshan Movement episodes I and II (~166.1 Ma), and the role of the Yanshan Movement episode II was gradually prominent [85]. The thrust nappe in the basin's western margin was strengthened, and the overall basin was continuously uplifted; however, the rising range in the basin's eastern part was much larger than that in the west, showing strong uplift and a denudation effect in the east and weak uplift in the west. Compared with the J_2z^1 period, the depocentre continued to migrate to the northwest of the basin and was located in the Qingcheng–Ansai area. The climate in this period became hot and arid, which was inconducive to plant growth and preservation.

The topographic elevation difference between the sedimentary area and the basin's periphery significantly reduced, and the sedimentary area became flatter. The sediment supply was insufficient. The sedimentary system included meandering river and lacustrine facies, and river deltas of different scales were deposited in the lake's entrance (Figure 8c). There is a clear differentiation of sedimentary facies in the basin. The basin's central part developed the fluvial delta facies, which transited into the catchment area of lacustrine facies to the east and southeast, and the other vast areas in the basin developed meandering river facies with high sinuosity. Because of seasonal flooding, the fine-grained sediments in the floodplain are widely deposited, but the sand bodies are isolated and have poor continuity. Affected by the downstream topography and lake scale, the meandering river's main channel bifurcates into multiple distributary channels in the delta plain. The clastic materials were transported along the distributary channel and distributed in a bird's foot shape and finally merged into the lake.

A small-scale lake developed in the basin's northeast-central region, the provenance came from the north, and the sediments were deposited relatively close to the provenance area, forming small meandering river deltas at the lake's catchment. The lakes extensively occur in the basin's south–southeast region, and the sediments came from the northwest and south areas, but the northwest area is the main provenance, and it was easy to form large-scale delta deposits at the catchment. The Qilian–Qinling Mountain and the southern margin of the North China block in the basin's south also provided some clastic materials, showing characteristics of near provenance, leading to the development of a small meandering river delta at the catchment.

After the above sedimentary filling evolution, the geographic distribution of the Zhiluo Formation becomes smaller than that of the Yan'an Formation, but it is still larger than that of the current basin. During this period, the sedimentary characteristics in the east and west of the basin were significantly differentiated, the uplift area in the eastern part expanded, and the depositional area shrank to the west and northwest. After the Zhiluo Formation's deposition, the basin experienced a short depositional discontinuity. Therefore, in the basin's peripheral areas, the contact relationship between the strata of the Zhiluo and Anding Formations shows parallel unconformity, but the basin's interior conforms [32].

5.3. Interrelationship between Tectonism, Climate and Sedimentation

In geological history, the tectonic movement of the lithosphere can change the paleogeomorphic pattern and affect the local/regional climate and atmospheric circulation [32,86–88], and the evolution of sedimentary sequences is the response to paleoclimate changes. For example, in the Cenozoic period, the convergence and collision between the Indian and Eurasian plates led to the overall uplift of the Qinghai–Tibet Plateau, which blocked the warm and humid airflow of the Indian Ocean into Asia's interior, making the climate hot and arid [89,90].

From the Late Triassic to Early and Middle Jurassic periods, the Ordos Basin had a considerable sedimentary area and a slight topographical elevation difference between the basin periphery and the sedimentary area [32,54], and the blocking effect of mountains on climate was not notable. During that period, the China continent was subjected to the closure of the Paleotethys Ocean and the subduction and collision of the Siberian plate [91,92], and under the combined southward and northward compression, coupled with the super monsoon, it significantly spread to the East Asian continent [32,93], leading to a warm and humid climate in North China (including Northeast China, North China and the Northwest China regions) [17,89]. In the late Yan'an Formation, the Ordos Basin's tectonic action changed from being controlled by the Tethys tectonic domain to being jointly controlled by the Tethys–Pacific tectonic domain [94], and its stress was gradually transformed from SN extrusion to NW–SE intracontinental compression deformation [93,95]. Compared with the Yan'an Formation, the Zhiluo Formation's CIA and ICV indexes have changed regulary, and both the bottom of $J_2z^{1\text{-}1}$ and J_2z^2 have changed suddenly; in $J_2z^{1\text{-}1}$, the CIA value at the bottom of the Zhiluo Formation decreased measurably, whereas the ICV value increased sharply; and in J_2z^2, the change frequency and range of the CIA and ICV indexes became more drastic [21,76] (Figure 6), indicating that the chemical weathering of the clastic material in the basin's peripheral area markedly weakened and the component maturity was significantly reduced, illustrating that the tectonic activity of the orogenic belt around the Ordos Basin strengthened in the early sedimentary stage of the Zhiluo Formation. This result is consistent with the widespread regional angular unconformity contact relationship between the Yan'an and Zhiluo Formations caused by the uplift of the Yanshan Movement episode I during this period [95].

During the $J_2z^{1\text{-}1}$ depositional period, the Ordos Basin was subjected to extensional stress after the late Yan'an Formation's uplift, and the entire basin subsided again at a rate of 0.6–1.6 m/Ma [96]. The super monsoon in this period affected northern China, and the basin's climate inherited the climatic characteristics of the Yan'an Formation and was dominated by a warm and humid environment [17,84,93]. The strong monsoon brought heavy rainfall, which promoted flourishing vegetation. Furthermore, the terrain elevation difference was still large, and the river's hydrodynamic force in the provenance was strong; therefore, the peripheral area provided sufficient sediments for the basin, suitable for forming the braided river sedimentary system. Then, a suite of a thick layer, containing many plant fossils and presenting a grey, grey-green medium-coarse grain braided river sedimentary system was widely deposited in $J_2z^{1\text{-}1}$, which was the sedimentary response to the climate and tectonism in this period.

In the $J_2z^{1\text{-}2}$ sedimentary period, the North China block was gradually uplifted due to the subduction and collision of the circum-Pacific plate into the Eurasian plate and the influence of the Paleotethys tectonic domain [54,97]. The Ordos Basin's western margin was characterised by weak overthrust, and the eastern part was slowly uplifted. Although the elevation difference in the Ordos Basin's paleotopography decreased, the uplift of the Qinling–Qilian orogenic belt in the basin's southern margin prevented the southern super monsoon from entering the basin. The weakening of the monsoon reduced rainfall and increased the temperature, causing the basin's climate to gradually change from warm and humid to semi-humid and semi-arid. Additionally, the smaller topographic elevation difference weakened the hydrodynamics of the rivers in the provenance area, decreasing the provenance supply capacity, and the sedimentary system was transformed from medium-

coarse-grained braided rivers to medium-fine-grained meandering rivers. The colour of rocks changed from grey and grey-green in the J_2z^{1-1} to grey and greyish-yellow mixed with purple and brown in the J_2z^{1-2}, and the increase in drought-tolerant plant types also corresponded to the hot and arid climate in this period.

During the J_2z^2 depositional period, the influence of the Paleotethys tectonism decreased, while the subduction and collision of the circum-Pacific plate to the Eurasian plate and the southward subduction of the Okhotsk Sea in the north significantly strengthened, causing a strong counterclockwise rotation of the basin's western margin under the action of left-lateral shear stress [97] and the continuous uplift of the entire basin. Affected by the above-mentioned tectonic transformation, the rising range in the basin's eastern part was much larger than in the western part, showing an uplift and denudation state of strong in the east and weak in the west, and the sedimentary centre further shifted to the northwest. The tectonic uplift's blocking effect on the climate in this period was clearly enhanced, making it challenging for the super monsoon to enter the basin. Furthermore, under the influence of the gradual formation of the planetary subtropical arid climate from east to west [98], coupled with the increasing global CO_2 concentrations and moving southward of the East Asian block by about 25° from the humid-temperate zone into the subtropical/tropical arid zone in the Northern Hemisphere, the climate in eastern and southern Asia, including Ordos Basin, became hot and arid [99,100]. As the basin's topography became flatter, rainfall decreased, hydrodynamics weakened, and sediment supply was insufficient. The sedimentary system was transformed from a low sinuous meandering river in the J_2z^{1-2} period to a high sinuous meandering river-delta-lake in J_2z^2. Furthermore, the commonly developed variegated fine-grained rocks (such as brown-red, purple-red and purple-brown) and a few plant fossils that were challenging to preserve embody the hot and arid climate.

Based on this evidence, the paleoclimate during the deposition time of the Middle Jurassic Zhiluo Formation in the Ordos Basin changed from warm and humid to hot and arid, constituting a good transition with the warm and humid climate of the Late Triassic–Early Jurassic period, proving that the transformation processes of the two tectonic domains in the Mesozoic were crucial to the changes in the paleoclimate and paleo-sedimentary environment in the Zhiluo Formation.

6. Conclusions

(1) During the Zhiluo Formation's depositional period, with the transition of paleoclimate from warm and humid to hot and arid, each member showed different characteristics in rock colour, composition, structure, plant fossils, spore and pollen assemblages and geochemistry. Vertically, the Zhiluo Formation's sedimentary facies was transformed from early braided rivers (braided river delta) to middle-meandering rivers and meandering river deltas, and lacustrine facies were later deposited in the basin's southeastern part.

(2) During the J_2z^{1-1} deposition period, the braided river delta facies was mainly distributed in the basin's northeast, and braided river facies were widely developed in the basin's northwest, west and south. The northwest and southwest basin margins of the basin in the J_2z^{1-2} period were still filled by braided river, and the braided river was transformed into the meandering river in the basin's interior and the depocentre located southeast of the current basin. During the J_2z^2 sedimentary period, the meandering river–meandering river delta-lacustrine facies developed successively from the basin margin to the interior, and the depocentre was located in the Ganquan-Ansai-Shenmu area. During the deposition of the Zhiluo Formation, the depocentre as a whole was characterized by gradual migration from southeast to northwest.

(3) In the J_2z^{1-1} sedimentary period, the southern super monsoon entered the basin and affected its climate, the strong monsoon brought heavy rainfall, the terrain elevation difference was large, and the peripheral area provided sufficient sediments, suitable for forming the braided river sedimentary system. During the J_2z^{1-2} depositional

period, the weakening of the monsoon reduced rainfall and increased the temperature, causing the basin's climate to change from warm and humid to semi-humid and semi-arid. What is more, due to the decline in the sediment supply capacity, the sedimentary system was transformed from braided rivers to meandering rivers. In the J_2z^2 sedimentary period, under the influence of the planetary subtropical arid climate, coupled with the increasing global CO_2 concentrations and moving southward of the East Asian block from the humid-temperate zone into the subtropical/tropical arid zone, the Ordos Basin became hot and arid climate, with decreased rainfall and insufficient sediment supply, and the meandering river-delta-lake sedimentary facies were developed.

Supplementary Materials: The following supporting information can be downloaded at: https://www.mdpi.com/article/10.3390/min13030314/s1, Figure S1: Major elements (%) and trace elements ($\times 10^{-6}$) content and ratios of Jurassic Zhiluo Formation mudstones in the Shenshangou area of Ordos Basin; Table S1: 15 outcrop sections of Zhiluo Formation in Ordos Basin.

Author Contributions: Conceptualization, L.C.; methodology, L.C.; writing—original draft preparation, L.C.; writing—review and editing, L.C., N.P. and D.Q.; supervision, Y.L. (Yongqing Liu); funding acquisition, N.P. and Y.L. (Yanxue Liu). All authors have read and agreed to the published version of the manuscript.

Funding: This study is financially supported by the Science and Technology Fundamental Resources Investigation Program (2022FY101800), the National Key Research and Development Program of China (2018YFC604201), the Program of National Natural Science Foundation of China (41672111, 42288201), the Program of China Geological Survey (DD20221649, DD20221786), and the International Geoscience Programme (IGCP675).

Data Availability Statement: The data are presented in the Supplementary File.

Acknowledgments: We thank Kuang Hongwei of the Chinese Academy of Geological Sciences for editing and reviewing this manuscript; Miao Peiseng, Li Jianguo and Chen Yin of the Tianjin Center of the China Geological Survey for their data assistance; and Hu Yongxing of the Geological Survey Institute of Gansu province for providing help with the core data.

Conflicts of Interest: The authors declare that they have no competing interests.

References

1. Deng, S.H.; Lu, Y.Z.; Fan, R.; Fang, L.H.; Li, X.; Liu, L. Toarcian (Early Jurassic) Oceanic Anoxic Event and the Responses in Terrestrial Ecological System. *Earth Sci. J. China Univ. Geosci.* **2012**, *37*, 23–38.
2. Huang, D.Y. Jurassic integrative stratigraphy and timescale of China. *Sci. China Earth Sci.* **2019**, *62*, 223–255. [CrossRef]
3. Chandler, M.A.; Rind, D.; Rucdy, R. Pangacan climate during the Early Jurassic: GCM simulations and the sedimentary record of palcoclimate. *Geol. Soc. Am. Bull.* **1992**, *104*, 543–559. [CrossRef]
4. Berner, R.A. GEOCARB II: A revised model of atmospheric CO2 over Phanerozoic time. *Am. J. Sci.* **1994**, *294*, 56–91. [CrossRef]
5. Sellwood, B.W.; Valdes, P.J. Jurassic climates. *Proc. Geol. Assoc.* **2008**, *119*, 5–17. [CrossRef]
6. Gröcke, D.R.; Hori, R.S.; Trabucho-Alexandre, J. An open marine record of the Toarcian oceanic anoxic event. *Solid Earth Discuss.* **2011**, *3*, 385–410.
7. Dera, G.; Brigaud, B.; Monna, F.; Laffont, R.; Puceat, E.; Deconinck, J.; Pellenard, P.; Joachimski, M.M.; Durlet, C. Climatic ups and downs in a disturbed Jurassic world. *Geology* **2011**, *39*, 215–218.
8. Gutjahr, M.; Ridgwell, A.; Sexton, P.F.; Anagnostou, E.; Pearson, P.N.; Pälike, H.; Norris, R.D.; Thomas, E.; Foster, G.L. Very large release of mostly volcanic carbon during the Palaeocene-Eocene Thermal Maximum. *Nature* **2017**, *548*, 573–577. [CrossRef]
9. Jenkyns, H.C.; Clayton, C.J. Lower Jurassic epicontinental carbonates and mudstones from England and Wales: Chemostratigraphic signals and the early Toarcian anoxic event. *Sedimentology* **1997**, *144*, 687–706. [CrossRef]
10. Guo, B.; Eleyb, Y.; Hiltonb, J.; Zoua, M.J.; Wang, Q.W. Carbon-isotope, petrological and floral record in coals: Implication for Bajocian (Middle Jurassic) climate change. *Int. J. Coal Geol.* **2020**, *220*, 103417.
11. Deconinck, J.F.; Hesselbo, S.P.; Pellenard, P. Climatic and sea-level control of Jurassic (Pliensbachian) clay mineral sedimentation in the Cardigan Bay Basin, Llanbedr (Mochras Farm) borehole, Wales. *Sedimentology* **2019**, *66*, 2769–2783. [CrossRef]
12. Dromart, G.; Garcia, J.P.; Picard, S. Ice age at the Middle-Late Jurassic transition? *Earth Planet. Sci. Lett.* **2003**, *213*, 205–220. [CrossRef]
13. Deng, S.H.; Yao, Y.M.; Ye, D.Q. *Jurassic System of North of China (I), Stratum Introduction*; Petroleum Industry Press: Beijing, China, 2003; pp. 1–339.

14. Li, S.P.; Liu, Y.Q.; Kuang, H.W.; Peng, N.; Jia, J.L.; Wang, T. Palynoflora from the Jurassic of Yingen−Ejin basin, NW China and its implications for the stratigraphy and geochronology-a case study on MED-1 drill core. *Acta Geol. Sin.* **2021**, *95*, 1382–1399.
15. Vakhrameyev, V.A. Classopollis pollen as an indicator of Jurassic and Cretaceous climate. *Internat. Geol. Rev.* **1982**, *24*, 1190–1196. [CrossRef]
16. Krassilov, V.A. *Hardin H. Paleoecology of Terrestrial Plants, Basic Principle and Techniques*; Wiley: New York, NY, USA, 1977; pp. 1–283.
17. Deng, S.H.; Lu, Y.Z.; Zhao, Y.; Fan, R.; Wang, Y.D.; Yang, X.J.; Li, X.; Sun, B.N. The Jurassic palaeoclimate regionalization and evolution of China. *Earth Sci. Front.* **2017**, *24*, 106–142.
18. Zhong, X.C. Ostracoda fossils of Upper Triassic and Middle Jurassic in Ordos Basin. *J. Paleontol.* **1964**, *12*, 426–466.
19. Jin, R.S.; Yu, R.A.; Yang, J.; Zhou, X.X.; Teng, X.M.; Wang, S.B.; Si, Q.H.; Zhu, Q.; Zhang, T.F. Paleo-environmental constraints on uranium mineralization in the Ordos Basin: Evidence from the color zoning of U-bearing rock series. *Ore Geol. Rev.* **2020**, *104*, 175–189. [CrossRef]
20. Zhou, Z.Y. Jurassic Floras. In *Fossil Floras of China through the Geological Ages*; Li, R., Ed.; Guangdong Science and Technology Press: Guangzhou, China, 1995; pp. 343–410.
21. Zhang, T.F.; Sun, L.X.; Zhang, Y. Geochemical characteristics of the Jurassic Yan'an and Zhiluo Formations in the northern margin of Ordos basin and their paleoenvironmental implications. *Acta Geol. Sin.* **2016**, *90*, 3454–3472.
22. Sun, L.X.; Zhang, Y.; Zhang, T.F.; Cheng, Y.H.; Li, Y.F.; Ma, H.L.; Yang, C.; Guo, J.C.; Lu, C.; Zhou, X.G. Jurassic Sporopollenin of Yan'an Formation and Zhiluo Formation in the northeastern Ordos Basin, Inner Mongolia, and its paleoclimatic significance. *Earth Sci. Front.* **2017**, *24*, 32–51.
23. Lei, K.Y.; Liu, C.y.; Zhang, L.; Li, B. Sedimentary provenance of Zhiluo Formation of the Middle southern Ordos Basin, evidence from palaeocurrent direction and U−Pb geochronology of detrital zircons. *Earth Sci. Front.* **2017**, *24*, 254–276.
24. Zhu, Q.; Li, J.G.; Miao, P.S. Reservoir Characteristics of Luohe Formation and Metallogenic Geological Conditions of Deep Uranium in the Southwestern Margin of Ordos Basin, China. *J. Earth Sci. Environ.* **2019**, *41*, 675–690.
25. Song, Y.; Hai, L.F.; Mei, C.; Ma, Y.P.; Li, H.F. The indication of ancient environment in the age of Lingwu dinosaurs based on plant fossils and sedimentary rocks in Zhiluo Formation Lingwu, Ningxia. *Sci. Technol. Eng.* **2020**, *20*, 10592–10597.
26. Cheng, S.T.; Huang, Y.Q.; Fu, X.H. Paleogeography Reconstruction of the Early-Middle Jurassic Large Ordos Basin and Development and Evolution of Continental Downwarping. *Acta Sedimentol. Sin.* **1997**, *15*, 43–49.
27. Zhang, K.; Zou, H.W.; Liu, Z.W.; Ma, Z.W. On the Jurassic West Boundary of the Ordos Basin. *Geol. Rev.* **2009**, *55*, 761–774.
28. Guo, Q.Y. Tectonic Evolution at the Western Margin of Ordos Basin with Respect to Metallogenesis of Sandstone Type Uranium Deposits. Ph.D. Dissertation, China University of Geosciences, Beijing, China, 2010; pp. 1–253.
29. Zhao, M.W.; Ahrendt, H.; Wemmer, K.; Behr, H.J. Silurian-Devonian and Jurassic Thermal events in the Ordos Basin, China: Evidence from K-Ar dating on illites. *Acta Geol. Sin.* **1996**, *70*, 186–194.
30. Li, Z.H.; Dong, S.W.; Feng, S.B.; Qu, H.J. Sedimentary response to Middle-Late Jurassic tectonic events inthe Ordos Basin. *Acta Geosci. Sin.* **2015**, *36*, 22–30.
31. Liu, C.Y. *Advances in the Accumulation and Formation for Multi-Energy Mineral Deposits Coexisting in the Same Basin*; Science Press: Beijing, China, 2015; pp. 1–25.
32. Liu, C.Y.; Zhao, H.G.; Zhao, J.F.; Wang, J.Q.; Zhang, D.D.; Yang, M.H. Temporospatial coordinates of evolution of the Ordos Basin and its mineralization responses. *Acta Geol. Sin.* **2006**, *82*, 1229–1243.
33. Chen, Y.X.; Dai, D.L.; Yang, C.G. *Research Methods of Lithofacies and Paleogeography*; Geological Publishing House: Beijing, China, 1981; pp. 96–115.
34. Xing, X.J.; Liu, Y.Q.; Fan, A.P. Genesis of sandstone-type uranium deposits:A case study in the Diantou area of the Ordos basin. *Geol. China* **2006**, *33*, 591–597.
35. Jiao, Y.Q.; Wu, L.Q.; Rong, H.; Peng, Y.B.; Miao, A.S.; Wang, X.M. The Relationship between Jurassic Coal Measures and Sandstone−type Uranium Deposits in the Northeastern Ordos Basin, China. *Acta Geol. Sin.* **2016**, *90*, 2117–2132. [CrossRef]
36. Wang, X.P.; Liu, K.P.; Chen, H.B.; Gong, B.L.; Yu, H.W.; Gong, Q.F.; Han, D. Sedimentary characteristics of the Jurassic Zhiluo Formation and uranium deposits in Zhiluo-Diantou area, southern Ordos Basin. *J. Paleogeogr.* **2020**, *22*, 295–307.
37. Lei, K.Y. Comparative Research on Sedimentary Characteristics and Provenance of Zhiluo Formation in the Northern Ordos Basin and Southern Ordos Basin. Master's Thesis, Northwest University, Xi'an, China, 2016.
38. Xue, R. Sedimentary Characteristics of the Jurassic Zhiluo Formation in Northern Ordos Basin and Implications for Uranium Mineralization. Master's Thesis, Northwest University, Xi'an, China, 2017.
39. Luo, W. Sedimentary Evolution and Provenance Analysis of the Middle Jurassic Zhiluo Formation in Majiatan-Huianbao Area, Western Ordos basin. Master's Thesis, Northwest University, Xi'an, China, 2017.
40. Yang, J.; Wang, S.B.; Liu, F. Sedimentary facies of the Zhiluo formation and its relationship with uranium mineralization in the Huanxian Area, west of Ordos Basin. *Sci. Technol. Eng.* **2019**, *19*, 64–70.
41. Yang, R.C.; Han, Z.Z.; Fan, A.P. Sedimentary microfacies and Ssequence stratigraphy of sandstone-type uranium deposit in the Dongsheng area of the Ordos basin. *J. Stratigr.* **2007**, *31*, 261–266.
42. Zhao, L. Sedimentary Characteristics and its Hydrogeological Significance of Jurassic ZhiLuo Formation in the east of Ningxia. Master's Thesis, Shandong University of Science and Technology, Qingdao, China, 2011.
43. Fan, A.P. Constraint on Diagenesis of Jurassic Sandstone Type Uranium Deposits in Dongsheng Area, Ordos Basin. Ph.D. Thesis, Northwest University, Xi'an, China, 2007.

44. Liu, H.Y. Geological structure characteristics and uranium metallogenic significance of Hangjinqi area in northern Ordos Basin. Master's Thesis, Northwest University, Xi'an, China, 2014.
45. Wu, Z.J.; Yan, M.H.; Han, X.Z.; Yu, R.A.; Sima, X.Z.; Jiang, Z.; Yin, D.F.; Hu, H.; Deng, Y.T. Uranium metallogenic characteristics and prospecting significance of Hongqingliang area in northeastern Ordos basin. *Coal Geol. Explor.* **2019**, *47*, 22–31.
46. Zhang, L.; Wu, B.L.; Liu, C.Y.; Lei, K.Y.; Hou, H.Q.; Sun, L.; Cun, X.N.; Wang, J.Q. Provenance analysis of the Zhiluo Formation in the sandstone-hosted uranium deposits of the northern Ordos Basin and implications for uranium mineralization. *Acta Geol. Sin.* **2016**, *90*, 3441–3453.
47. Zhao, J.F.; Liu, C.Y.; Yu, L.; Huang, L.; Liu, Y.T.; Gao, F. Distributional and sedimentary characteristics of sandstones in Jurassic Zhiluo Formation, Ordos Basin. *Acta Sedimentol. Sin.* **2007**, *25*, 535–544.
48. Zhao, J.F.; Liu, C.Y.; Zhao, J.S. Sedimentary facies and its evolution of Jurassic Zhiluo Formation in Ordos basin. *J. Northwest Univ.* **2008**, *38*, 480–486.
49. Zhao, J.F.; Liu, C.Y.; Liang, J.W.; Wang, X.M.; Yu, L.; Huang, L.; Liu, Y.T. Restoration of the original sedimentary boundary of the middle Jurassic Zhiluo Formation-Anding Formation in the Ordos Basin. *Acta Geol. Sin.* **2010**, *84*, 553–569.
50. Scotese, C.R. *Atlas of Jurassic Paleogeographic Maps, PALEOMAP Atlas for ArcGIS, 3: The Jurassic and Triassic, Maps 32–42, Mollweide Projection, Paleomap Project, Evanston, IL*; Qualit: Luxemburg, WI, USA, 2014.
51. Gao, X.Y.; Zhao, T.P. Late Mesozoic magmatism and tectonic evolution in the Southern margin of the North China craton. *Sci. China Earth Sci.* **2017**, *60*, 1959–1975. [CrossRef]
52. Cheng, Y.Q.; Geng, S.F.; Xie, L.Z. *1:5 Million Geological Map of China*; 2nd ed.; Geological Publishing House: Beijing, China, 2002.
53. Chen, Y.; Feng, X.X.; Chen, L.L.; Jin, R.S.; Miao, P.S.; Sima, X.Z.; Miao, A.S.; Tang, C.; Wang, G.; Liu, Z.R. Ananalysis of U-Pb dating of detrital zircons and modes of occurrence of uranium minerals in the Zhiluo Formation of northeastern Ordos Basin and their indication to uranium sources. *Geol. China* **2017**, *44*, 1190–1206.
54. Zhao, J.F.; Liu, C.Y.; Huang, L.; Zhang, D.D.; Wang, D.; Wang, D. Paleogeography reconstruction of a multi–stage modified intracratonic basin–a case study from the Jurassic Ordos Basin, Western North China Craton. *J. Asian Earth Sci.* **2020**, *190*, 104191. [CrossRef]
55. Wang, Z.T.; Zhou, H.R.; Wang, X.L.; Jing, X.C. Characteristics of the crystalline basement beneath the Ordos Basin: Constraint from aeromagnetic data. *Geosci. Front.* **2015**, *6*, 465–475. [CrossRef]
56. Deng, J.; Wang, Q.F.; Gao, B.F.; Huang, D.H.; Yang, L.Q.; Xu, H.; Zhou, Y.H. Evolution of the Ordos Basin and its distribution of various energy and mineral resources. *Geoscience* **2005**, *19*, 538–545.
57. Ritts, B.D.; Hanson, A.D.; Darby, B.J.; Nanson, L.; Berry, A. Sedimentaryrecord of Triassic intraplate extension in North China: Evidence from the nonmarine NW Ordos Basin, Helan Shan and Zhuozi Shan. *Tectonophysics* **2004**, *386*, 177–202. [CrossRef]
58. Jiang, L.; Qiu, Z.; Wang, Q.C.; Guo, Y.S.; Wu, C.F.; Wu, Z.J.; Xue, Z.H. Joint development and tectonic stress field evolution in the southeastern Mesozoic Ordos Basin, west part of North China. *J. Asian Earth Sci.* **2016**, *127*, 47–62. [CrossRef]
59. Liu, C.Y.; Wang, J.Q.; Zhang, D.D.; Zhao, H.G.; Zhao, J.F.; Huang, L.; Wang, W.Q.; Qin, Y. Genesis of rich hydrocarbon resources and their occurrence and accumulation characteristics in the Ordos Basin. *Oil Gas Geol.* **2021**, *42*, 1011–1029.
60. Yang, J.; Li, K.; Zhang, D.; Zhang, S.; Liu, S. Petroleum Geology of China. In *Changqing Oil Field*; Petroleum Industry Press: Beijing, China, 1992; Volume 12, pp. 1–490.
61. Chen, L.L.; Feng, X.X.; Sima, X.Z.; Li, J.G.; Guo, H.; Chen, Y.; Zhao, H.L.; Tang, C.; Wang, G.; Liu, Z.R.; et al. Occurrence Forms of the Uranium Minerals in the Nalinggou Area of the Ordos Basin and Geological Implications. *Geol. Explor.* **2017**, *53*, 632–642.
62. Cao, H.F.; Liu, H.N.; Du, P.; Peng, X.H. Characteristics of Shuanglong Uranium Deposit and the Types of Uranium Mineral in the Southern Margin of Ordos Basin. *Geol. Sci. Technol. Inf.* **2018**, *37*, 148–153.
63. Sun, Z.; Xie, Q.; Yang, J. Ordos Basin a typical example of an unstable cratonic interior superimposed basin. In *Chinese Sedimentary Basins*; Zhu, X., Ed.; Petroleum Industry Press: Beijing, China, 1989; pp. 63–75.
64. Li, S.G.; Ge, N.; Liu, D.; Zhang, Z.; Ye, X.; Zheng, S.; Peng, C. The Sm-Nd isotopic age of C–type eclogite from Dabie Group in the Northern Dabie Mountains and its tectonic implication. *Chin. Sci. Bull.* **1989**, *34*, 1623–1628.
65. Shao, S.Z. Study on Jurassic Sedimentary System and Main Sand Bodies in Yulin–Yan'an Area. Ordos Basin. Master's Thesis, China University of Geoscience, Beijing, China, 2005.
66. Liu, S.; Yang, S. Upper Triassic-Jurassic sequence stratigraphy and its structural controls in the western Ordos basin, China. *Basin Res.* **2000**, *12*, 1–18. [CrossRef]
67. Liu, Y.Q.; Kuang, H.W.; Peng, N.; Xu, H.; Zhang, P.; Wang, N.S.; An, W. Mesozoic basins and associated palaeogeographic evolution in North China. *J. Palaeogeogr.* **2015**, *4*, 189–202. [CrossRef]
68. Jin, J.Q.; Zhao, W.Z.; Xue, L.Q.; Meng, Q.R. Proto−Types and Evolution of Jurassic Basins in NW China. *Geol. Rev.* **1999**, *45*, 92–104.
69. Xu, X.H.; Huang, Z.G.; Gao, C.L.; Zhang, Y.C. Diktyogenese and basins in China continent during the Mesozoic−Cenozoic. *Pet. Geol. Exp.* **2009**, *31*, 119–127.
70. Liu, C.Y.; Zhao, H.G.; Gui, X.J.; Yue, L.P.; Zhao, J.F.; Wang, J.Q. Space−Time Coordinate of the Evolution and Reformation and Mineralization Response in Ordos Basin. *Acta Geol. Sin.* **2006**, *80*, 617–638.
71. Zhang, Y.; Sun, L.X.; Zhang, T.F.; Cheng, Y.H.; Li, Y.F.; Ma, H.L.; Lu, C.; Yang, C.; Guo, J.C.; Zhou, X.G. Sequence stratigraphy study of coal uranium bearing rock series and occurrence regularity coal and uranium in the northeastern margin of Ordos Basin. *Acta Geol. Sin.* **2016**, *90*, 3424–3440.

72. Xie, X.Y. Provenance and sediment dispersal of the Triassic Yanchang Formation, southwest Ordos Basin, China, and its implications. *Sediment. Geol.* **2016**, *335*, 1–16. [CrossRef]
73. Xue, R.; Zhao, J.f.; Yan, Z.d. Sedimentary characteristics and evolution of the Jurassic Zhiluo Formation in northern Ordos basin. *J. Palaeogeogr.* **2017**, *19*, 999–1012.
74. Jiao, Y.Q.; Chen, A.P.; Wang, M.F. Genetic analysis of the bottom sandstone of Zhiluo Formation, northeastern Ordos basin: Predictive base of spatial orientation of sandstone-type uranium deposit. *Acta Sedimentol. Sin.* **2005**, *23*, 371–379.
75. He, X.L. Depositional Environment of Zhiluo Formation in Fuxian Shanxi Province. Master's Thesis, Chang'an University, Xi'an, China, 2015.
76. Cui, L.W.; Peng, N.; Liu, Y.Q.; Qiao, D.W.; Liu, Y.X. Detrital Zircon Geochronology and Tectonic Evolution Implication of the Middle Jurassic Zhiluo Formation, Southern Ordos Basin, China. *Minerals* **2023**, *13*, 45. [CrossRef]
77. Nesbitt, H.W.; Young, G.M. Early Proterozoic climates and plate motions inferred from major element chemistry of lutites. *Nature* **1982**, *299*, 715–717. [CrossRef]
78. Cullers, R.L. The controls on the major-and trace-element evolution of shales, siltstones and sandstones of Ordovician to Tertiary age in the Wet Mountains region, Colorado, U.S.A. *Chem. Geol.* **1995**, *123*, 107–131. [CrossRef]
79. Liu, G.; Zhou, D.S. Application of micro elements analysis in identifying sedimentary environment. *Pet. Geol. Exp.* **2007**, *29*, 307–314.
80. Lermanm, A. *Lakes: Chemistry, Geology, Physics*; Springer: Berlin/Heidelberg, Germany, 1978; pp. 79–83.
81. Chen, J.; Wang, Y.J.; Chen, Y.; Liu, L.W.; Ji, J.F.; Lu, H.Y. Rb and Sr geochemical characterization of the Chinese loess and its implications for palaeomonsoon climate. *Acta Geol. Sin.* **2001**, *75*, 259–266.
82. Wu, R.G.; Chen, A.P.; Yu, D.G.; Zhu, M.Q.; Zhou, W.P. Analysis on depositional system and discussion on ore formation conditions of channel sandstone type uranium deposit–taking Dongsheng area, Ordos Mesozoic basin as an example. *Uranium Geol.* **2003**, *19*, 94–99.
83. Miao, Z.L.; Zhu, L.J.; Hou, M.C.; Chen, A.Q.; Luo, W.; Shi, X.; Wang, H.H.; Liu, Y.C.; Wang, L.G. Edimentary fades of Middle Jurassic Zhiluo Formation in Yanwu area, Ordos Basin. *J. Chengdu Univ. Technol.* **2018**, *45*, 166–176.
84. Zhang, T.F.; Zhang, Y.; Jin, R.S.; Yu, R.A.; Sun, L.X.; Cheng, Y.H.; Ao, C.; Ma, H.L. Characteristics of Jurassic sequence boundary surfaces on the northeastern margin of Ordos basin and their constraints on the spatial-temporal properties of sandstone uranium mineralization. *Geol. China* **2020**, *47*, 278–299.
85. Li, B.X.; Xu, F.X.; Ma, Q.H.; Pan, H.Z.; Wang, S.Q.; Li, Z.W. Middle Jurassic strata in Wangjiashan basin, Jingyuan, Gansu Province. *J. Stratigr.* **1982**, *1*, 33–40.
86. Dai, G.L.; Yang, T.; Zhou, Y.; Niu, C. Exploration of the water-abundant sandstone geological features of Ningtiaota Ida Nao Luo in Shenfu mining area. *J. Saf. Environ.* **2016**, *16*, 144–148.
87. West, A.J.; Galy, A.; Bickle, M. Tectonic and climatic controls on silicate weathering. *Earth Planet. Sci. Lett.* **2005**, *235*, 211–228. [CrossRef]
88. Liu, J.; Zhang, J.Y.; Ge, Y.K. Tectonic geomorphology: An interdisciplinary study of the interaction among tectonic climatic and surface processes. *Chin. Sci. Bull.* **2018**, *63*, 3070–3088. (In Chinese)
89. Chen, P.R.; XU, Z.J.; Kong, J.T.; Cheng, R.H. Paleoclimatic Evolution During Middle Jurassic in Southwestern Fujian and its Responses to the Tectonic Regime Transition in South China. *Geotecton. Metallog.* **2020**, *44*, 1012–1024.
90. Abels, H.A.; Dupont-Nivet, G.; Xiao, G.; Bosboom, R.; Krijgsman, W. Step-wise change of Asian interior climate preceding the Eocene-Oligocene Transition (EOT). *Palaeogeogr. Palaeoclimatol. Palaeoecol.* **2011**, *299*, 399–412. [CrossRef]
91. Xing, G.F.; Lu, Q.D.; Chen, R.; Zhang, Z.Y.; Nie, T.C.; Li, L.M.; Huang, J.L.; Lin, M. Study on the Ending Time of Late Mesozoic Tectonic Regime Transition in South China-Comparing to the Yanshan Area in North China. *Acta Geol. Sin.* **2008**, *82*, 451–463.
92. Li, S.Z.; Zang, Y.B.; Wang, P.C.; Suo, Y.H.; Li, X.Y.; Liu, X.; Zhou, Z.Z.; Liu, X.G.; Wang, Q. Mesozoic tectonic transition in South China and initiation of Palaeo-Pacific subduction. *Earth Sci. Front.* **2017**, *24*, 213–225.
93. Liu, C.L.; Wu, C.H.; Wang, L.C.; Fang, X.M.; Zhao, Y.J.; Yan, M.D.; Zhang, Y.S.; Cao, Y.T.; Zhang, H.; Lü, F.L. Advance in the Study of Forming Condition and Prediction of Potash Deposits of Marine Basins in China's Small Blocks: Review. *Acta Geosci. Sin.* **2016**, *37*, 581–606.
94. Wang, Y. *Evolution and Dynamics of Orogenic Belts and Basins in North China since Mesozoic*; Geological Publishing House: Beijing, China, 1998.
95. Wu, Z.J.; Han, X.Z.; Lin, Z.X.; Li, Z.N.; Ji, H.; Yin, D.F.; Jiang, Z.; Hu, H. Tectonic, Sedimentary, and Climate Evolution of Meso-Cenozoic Basins in North China and its Significance of Coal Accumulation and Uranium Mineralization. *Geotecton. Metallog.* **2020**, *44*, 710–724.
96. Yang, H.; Li, X.S.; Yan, X.X. The relationship between tectonic sedimentary evolution and tight sandstone gas reservoir since the late Paleozoic in Ordos Basin. *Earth Sci. Front.* **2015**, *22*, 174–183.
97. Yang, S.B.; Geng, X.X.; Guo, Q.Y.; Hou, G.T.; Liu, Z.B. Mesozoic Tectonic Evolution in North Section of the Western Margin of Ordos basin. *Geol. Rev.* **2008**, *54*, 307–315.
98. Wang, P.X. Global monsoon in a geological perspective. *Chin. Sci. Bull.* **2009**, *54*, 1113–1136. [CrossRef]

99. Boucot, A.J.; Gray, J. A critique of Phanerozoic climatic models involving changes in the CO_2 content of the atmosphere. *Earth-Sci. Rev.* **2001**, *56*, 1–159.
100. Yi, Z.Y.; Liu, Y.Q.; Meert, J.G. A true polar wander trigger for the Great Jurassic East Asian Aridification. *Geology* **2019**, *47*, 1112–1116. [CrossRef]

Disclaimer/Publisher's Note: The statements, opinions and data contained in all publications are solely those of the individual author(s) and contributor(s) and not of MDPI and/or the editor(s). MDPI and/or the editor(s) disclaim responsibility for any injury to people or property resulting from any ideas, methods, instructions or products referred to in the content.